THE TOTAL CROSS SECTION FOR FAST NEUTRONS OF N^{14}

by

WERNER KUBELKA

A THESIS SUBMITTED IN PARTIAL FULFILMENT OF THE REQUIREMENTS FOR THE DEGREE OF MASTER OF SCIENCE

in the Department

of

Physics

We accept this thesis as conforming to the standard required from candidates for the degree of MASTER OF SCIENCE

Members of the Department of Physics

THE UNIVERSITY OF BRITISH COLUMBIA

April, 1955

A B S T R A C T

THE TOTAL CROSS SECTION FOR FAST NEUTRONS OF N^{14}

The total neutron cross section of N^{14} was measured for neutron energies from 3.6 to 4 Mev. A 15-cm.-long liquid Nitrogen cell was irradiated with monochromatic neutrons from the D(d,n)He reaction, going in energy steps of approximately 15 kev. The transmission was measured at each energy, using a propane recoil counter for counting the transmitted neutrons. An identical counter was used at 90° for monitoring. The results appear to confirm Stetter and Bothe's measurements, which were made with a continuous neutron energy distribution.

ACKNOWLEDGEMENTS

The author wishes to express his thanks to Drs. J.B. Warren and D.B. James, who suggested this project, and encouraged it with suggestions and patience. Thanks are also due to Dr. James and Mr. Y.I. Ssu, for spending long days and nights with the author at the Van de Graaf machine, when the measurements were taken.

CONTENTS

INTRODUCTION

The many possible interactions of neutrons with nuclei are expressed in terms of cross sections, σ square cm, for the various interactions, where σ may be visualized as an effective target area offered by the nucleus to an incident neutron beam. If a neutron passes normally through a thin sheet of material, area A, thickness t, containing N nuclei per cm^3, the chance of a collision will be

$$\frac{\text{No of target nuclei} \times \sigma}{A} = \frac{Nt\sigma}{1}$$

since the overlapping of nuclear areas is negligible. Thus for an incident beam of n neutrons per cm^3 moving with a velocity v the collisions per cm^2 per second will be

$$n.v. \frac{\text{No of target nuclei} \times \sigma}{A} = n.v.Nt.\sigma$$

or

$$\sigma = \frac{\text{collisions per } cm^3 \text{ per seonnd}}{n.v.N} \quad \ldots(1)$$

Thus where the interaction rate per cm^3 does not depend on the neutron energy, the cross section is inversely proportional to the velocity of the neutrons.

The variety of ways in which a neutron of an energy between a few ev. and 20 Mev. may interact with nuclei may be conveniently grouped under following processes. In the first place the neutron may be scattered elastically without loss of kinetic energy, as for example in the case $N^{14}(n,n)N^{14}$. Secondly the neutron, after entering the nucleus and forming

a compound nucleus, may be ejected with a lower energy, the nucleus being left in an excited state, e.g. $N^{14}(n,n')N^{14*}$. This is an inelastic scattering process, in which the surplus energy is emitted subsequently as a gamma ray. The compound nucleus, if formed in a state with adequate energy, may break up with the emission of charged particles, such as protons or alpha particles, or an additional neutron, e.g. $N^{14}(n,p)C^{14}$, $N^{14}(n,\alpha)B^{12}$, and (n,2n) processes. Again, the neutron may be captured and the surplus energy emitted as a gamma ray, e.g. $N^{14}(n,\gamma)N^{15}$, a process obviously favoured at low incident neutron energies. Finally there is the fission process, in which the compound nucleus may break up into two roughly equal fragments.

All these processes may contribute to the "total cross section" of the nuclei for removal of neutrons from a parallel monokinetic beam. However, a characteristic feature of neutron induced reactions is the existence of a well defined total cross section, which is essentially the sum of the elastic scattering and the reaction cross sections, and is relatively easy to measure. This is in contrast to the situation for charged particles, where the total cross section is ill defined, as the Rutherford scattering at low angles becomes large and is determined by the Coulomb forces far outside the nuclear radius.

For fast neutrons, 10 to 20 Mev, the total cross section is around $2\pi R^2$ for all nuclei, where R is the nuclear radius, πR^2 arising from the finite size of the nucleus

($R \gg \lambda$, the de Broglie wavelength of the incident neutron), and πR^2 from the diffraction or shadow by the nucleus of the neutron waves, i.e. $\sigma_{capture}$ of a neutron and $\sigma_{scattering}$ respectively. For neutrons of energy below a few hundred kev the elastic scattering and capture processes are predominant. Both show very characteristic resonance behaviour at similar energies, the resonance character of the capture process with slow neutrons being especially striking with heavy nuclei and being superimposed on a general $\frac{1}{v}$ dependance expected from equation (1). In the moderate energy region of a few Mev the formation of the compound nucleus may be followed by a variety of processes such as emission of charged particles, inelastic scattering etc., which are in competition. The major process in this region is naturally inelastic scattering, since the re-emission of a neutron is more probable than that of a charged particle, particularly from high Z nuclei. The general behaviour of the total cross section σ_t will be similar therefore to the cross section for the formation of the compound nucleus, rising slowly from πR^2 at high neutron energies proportionally to $\pi(R + \lambda\!\!\!^{-})^2$ at lower energies, with possible resonances superimposed, and the contribution of the elastic scattering cross section from the 'hard sphere' scattering, which is approximately πR^2.

The presence of resonances in the neutron cross section is interpreted as arising from the presence of stationary, quantized, energy levels of the compound nucleus. The width, magnitude and general shape of the resonances may be expressed

by the Breit Wigner formula to a high degree of accuracy, and involves the angular momentum of the excited state.

In the present work the total fast neutron cross section of a rather low Z nucleus, N^{14}, has been started over the energy region from 3 to 4 Mev, in which the (n,p) and (n,α) processes can compete favourably with the (n,n) processes. The neutron energy region up to 1.8 Mev has previously been carefully examined and shows several resonances. In this manner one might expect to find resonances arising from levels in N^{15} at the excitation corresponding to the incident neutron energy, and if so, to resolve the cross section into its component parts to determine which process was contributing.

I. THE TRANSMISSION EXPERIMENT

1. Fundamentals.

Charged particles, because of their charge, have definite ranges, and may therefore be stopped completely by absorbers, while neutrons and gamma rays can be diminished in numbers only, but never completely stopped. Thus the absorption of neutrons when passing through a material is completely determined by the chance that each individual particle either passes through unharmed, or interacts with a nucleus of the absorber. Consider an area of 1 cm^2 of an absorber of thickness x, and let $I = nv$ be the intensity of the incident neutrons striking this area. If N is the number of target nuclei per cm^3, then the number present in a thin layer dx will be Ndx nuclei per cm^2. From equation (1) it can be seen that the number of neutrons that will interact with such a layer will be $nvNdx\sigma = INdx\sigma$. As the number of neutrons that interact must be equal to the decrease of neutron intensity,

$$INdx\sigma = -dI$$

or

$$\frac{dI}{I} = -N\sigma dx$$

Integrating over the thickness x of the material,

$$\frac{I}{I_o} = e^{-N\sigma x}$$

and substituting $I = nv$,

$$\frac{n}{n_o} = e^{-N\sigma x} = T \qquad \text{.....(2)}$$

T is generally referred to as the transmission coefficient, since it represents the fraction of particles transmitted. The measurement of T is the most direct way of obtaining the total neutron cross section of a substance. It provides us with an absolute value of the cross section for each neutron energy under investigation, and therefore diminishes the likelihood of additive errors.

2. Difficulties and Corrections.

In principle the transmission experiment is very simple. The absorber is bombarded with neutrons, and the number of neutrons transmitted is counted. The cross section is then calculated from equation (2). In practice, however, many difficulties have to be overcome before reliable cross section values are obtained.

Generally it is desired to know the energy dependence of the cross section, and therefore an artificial neutron source has to be used to obtain monokinetic neutrons. Unfortunately the intensity of artificially produced neutron beams is not constant with time, thus some reference is needed to indicate the relative intensity of the beam. This can be done either by measuring the current on to the neutron producing target; or by having a monitor counter, counting either the neutrons emitted at a different angle, or some other particles leaving the target as a byproduct of the neutron producing reaction. If there exists any doubt as to whether the target thickness is uniform, a monitor counter should be used rather

than a "current integrator", because with nonuniform thickness a slight shift in beam position might result in a different target yield. Using a monitor counter or a current integrator, the transmission coefficient can be calculated from

$$T = \frac{r}{r_o} \qquad \text{.....(3)}$$

where r is the ratio of counts over monitor counts with the absorber in place, and r_o is the ratio of counts over monitor counts with the absorber removed.

Background counts of both scattered neutrons and gamma rays are always present when the neutrons are produced by particle accelerators. By proper selection of the detector it is possible to keep the gamma pulses sufficiently small, so that they may be biased out electronically. A large portion of the counts due to scattered neutrons can also be suppressed by means of biasing. However there will generally be some amounts of hydrogenous material present to scatter fast neutrons into the counter, and these neutrons may have energies comparable to that of the desired neutrons. Ricamo (1951), and Ricamo and Zünti (1951) showed that these undesired neutrons can be corrected for by means of a third measurement, using an absorber of known transmission coefficient, T'. If r_2 is the counting ratio for the known absorber and r_1 the counting ratio for the unknown absorber, then the transmission coefficient for the unknown absorber will be

$$T = 1 - (1 - T') \frac{r_o - r_1}{r_o - r_2} \qquad \text{.....(4)}$$

Generally T' is kept as small as possible so that uncertainties

in T' do not influence T significantly. If T' can be made small enough to be neglected, equation (4) becomes

$$T = \frac{r_1 - r_2}{r_o - r_2} \qquad \text{.....(5)}$$

In addition to the scattered neutrons, which are more or less continuous in energy distribution, monoenergetic neutrons, which are of other than the desired energy, may come from the source. Such "parasitic" neutrons may be a byproduct of the target reaction, or they may be caused by interaction of the ion beam with some other nucleus which is present on the target, or in its vicinity. In both cases the energy of the parasitic component will vary with the energy of the ion beam, and therefore with the energy of the neutrons. If the component if fairly strong, not only erroneous cross section values may be measured, but also resonances may be observed at a wrong place of the energy scale. If the component is not a byproduct of the target reaction, and its energy is too high to be biased out without sacrificing too much counter efficiency, everything possible should be tried to eliminate its source. If this is not possible or if the component is a byproduct of the target reaction, then the component must be accounted for, and equation (4) will take the form

$$T = 1 - (1 - T') \frac{r_o - r_1 - p(1 - t)}{r_o - r_2 - p(1 - t')} \qquad \text{.....(6)}$$

where p is the counting ratio of the parasitic component, and t and t' the corresponding transmissions. The determination of p will depend on its origin. If p is a byproduct of the target reaction it should be possible to find its strength

To follow page 4

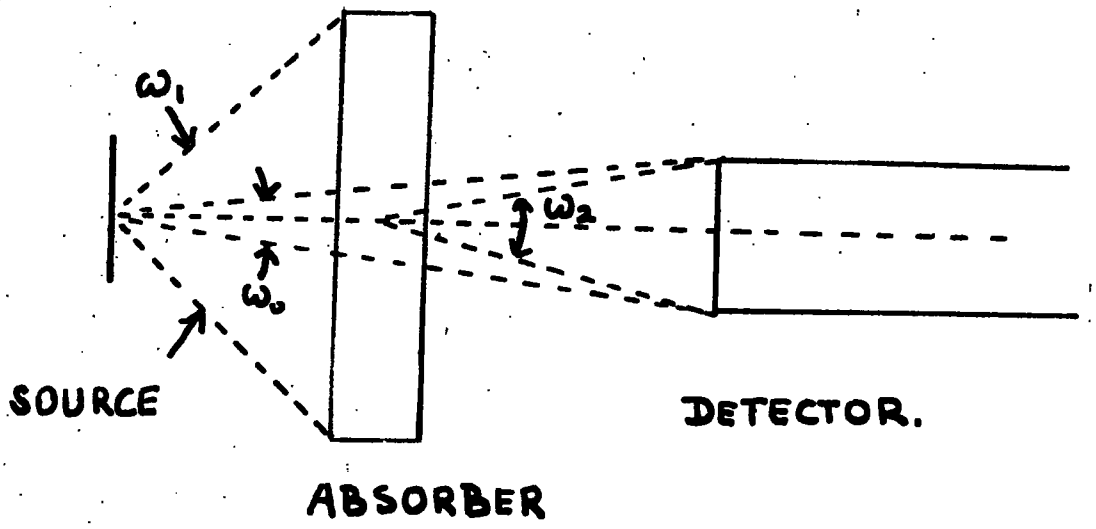

FIG. 1. Geometry of the Transmission Experiment.

relative to the desired component in the literature on that reaction. If p is originated by some other reaction its relative strength may be found by measuring the counting ratio for the same amount of integrator counts, with and without the target in place. The relative energy also may be found either from the literature or by measurement with no target present. t' will generally be available, as an absorber should be chosen for which the transmission coefficient is known over a wide range of energies. t can be estimated from transmission or cross section values either from the work under investigation or from work done by other authors, depending on the energy range of the parasitic component.

Another source of unwanted neutrons in the detector may be the absorber itself. Due to its finite size the absorber will scatter some neutrons into the counter. This "in scattering" may be minimized by keeping both counter and absorber as small as possible in area. Its effect on the transmission coefficient may be calculated from

$$T_o = T + (1 - T)G \qquad \ldots\ldots\ldots(7)$$

where T_o is the true, and T the apparent transmission. The geometrical factor G is given by

$$G = \frac{\omega_1 \omega_2}{4\pi\omega_o} \qquad \ldots\ldots\ldots(8)$$

The solid angles involved here are illustrated on Fig. 1.

The problem of the choice of the thickness of the absorber, and therefore the choice of T, was investigated by Rose and Shapiro (1948) and by Ricamo (1951). These authors say the optimal T lies between 0.2 and 0.3. Most authors,

however, prefer T > 0.5, so as to ensure that there is no multiple scattering in the absorber.

The physical and chemical constitution of the absorber must be carefully chosen. To calculate the cross section from the transmission, the number of nuclei per cm^2 must be known, and this depends on the density. Inhomogenity may therefore be a source of error, especially since only the average density can be measured. If the absorber is a chemical compound, other atoms will be present, and their cross section must be corrected for. It is therefore of advantage to use the absorbers in liquid form.

The use of liquid absorbers will also prove of advantage in another respect. The geometrical form and relative density distribution of the two absorbers should be identical, and the spacial distribution and relative intensity of source and background should not change during the course of the experiment. Liquid absorbers, in identical containers, will help to meet these requirements.

The statistical error of the cross section for the case of equation (5) was calculated by Ricamo (1951), and found to be

$$\frac{\Delta\sigma}{\sigma} = \left[\left(\frac{\Delta r_o}{r_o - r_1}\right)^2 + \left(\frac{\Delta r_1}{r_1 - r_2}\right)^2 + \left(\frac{\Delta r_2 (r_o - r_1)}{(r_1 - r_2)(r_o - r_2)}\right)^2\right]^{\frac{1}{2}} \quad \ldots(9)$$

where r_o, r_1 and r_2 are the respective statistical errors of the counting ratios.

II. THEORETICAL CONSIDERATIONS

1. Application of the Breit-Wigner Theory to N^{14}.

The nuclear reactions taking place when neutrons are absorbed by N^{14} are

$$n + N^{14} \longrightarrow N^{15} \longrightarrow C^{14} + p$$
$$\longrightarrow B^{11} + \alpha$$
$$\longrightarrow N^{14} + n$$

The application to nitrogen of the Breit-Wigner theory, as presented by Feshbach, Peaslee and Weisskopf (1947), Blatt and Weisskopf (1952) and Feld et al. (1951), is well illustrated by Hinchley, Stelson and Preston (1952), and by Johnson, Patree and Adair (1951).

Considering the reaction

a	+	A	$\longrightarrow$	C	$\longrightarrow$	B	+	b
bomb.part. ang mom.ℓ spin i wave length $2\pi\lambda_a$		target nucleus spin I		compound nucleus in state of spin J		residual nucleus spin I'		outg.part. ang.mom. spin i'ℓ'

the maximum value of the cross section at the resonance corresponding to the formation of C in the state of spin J will be given by

$$S_J^{\ell}(a,b) = 4\pi\lambda^2_a(2\ell+1)g_J^{\ell}\frac{\Gamma_a^{\ell}\Gamma_b^{\ell'}}{\Gamma^2} \quad \text{.....(10)}$$

where Γ_a^{ℓ} and $\Gamma_b^{\ell'}$ are the partial widths for the emission of the particles a and b from the compound nucleus respectively, and Γ is the total width of the resonance J. g_J^{ℓ} is the statistical weight factor and is given by

$$g_J^{\ell} = \frac{(2J + 1)}{(2i + 1)(2I + 1)(2\ell + 1)} \qquad \text{.....(11)}$$

This gives for the maximum cross section of the $N^{14}(n,n)N^{14}$ reaction, i.e. elastic scattering,

$$S_J(n,n) = 4\pi\lambda\!\!\!^{-2}_n \frac{(2J + 1)}{2(2I + 1)} \gamma^2 \qquad \text{.....(12)}$$

where $\gamma = \frac{\Gamma_n}{\Gamma}$

On the other hand from equation (10) for the $(n\alpha)$ and (n,p) reactions

$$S_J(n,p) + S(n,\alpha) = 4\pi\lambda\!\!\!^{-2} \frac{2J + 1}{6} \left[\frac{\Gamma_n\Gamma_p + \Gamma_n\Gamma_\alpha}{\Gamma^2}\right] \qquad \text{....(13)}$$

Using the definitions of $\gamma = \frac{\Gamma_n}{\Gamma}$ and $\Gamma = \Gamma_n + \Gamma_\alpha + \Gamma_p$ the expression in square brackets in equation (13) becomes

$$\frac{\Gamma_n\Gamma_p + \Gamma_n\Gamma_\alpha}{\Gamma^2} = \frac{\Gamma_n}{\Gamma}\left(\frac{\Gamma_p + \Gamma_\alpha + \Gamma_n}{\Gamma} - \frac{\Gamma_n}{\Gamma}\right) = \gamma(1 - \gamma)$$

and γ can be evaluated with the help of equation (13) as

$$\gamma(1 - \gamma) = \frac{S_J(n,p) + S_J(n,\alpha)}{4\pi\lambda\!\!\!^{-2} \frac{1}{6}(2J + 1)} \qquad \text{.....(14)}$$

If there would be a "hard" nucleus, i.e. if the nucleus could be considered as a perfectly reflecting sphere, there would be only one type of scattering, the "potential" scattering, which is given by

$$\sigma_{pot} = 4\pi\lambda\!\!\!^{-2}(2\ell + 1)\sin^2\delta_e \qquad \text{.....(15)}$$

where the phase constants, δ_e, are given by

$$\delta_0 = x$$

$$\delta_1 = x - \frac{1}{2}\pi + \cos^{-1}x$$

$$\delta_2 = x = \pi^2 + \cos^{-1}\left[\frac{x^2 - 3}{3x}\right]$$

x being $x = \frac{R}{\lambda\!\!\!^{-}_n}$ (R is the nuclear radius). This, combined with

the cross section due to the (n,n) reaction will give the total elastic scattering as

$$S^{\ell}_{J\,tot.}(n,n) = S_{J\,reaction}(n,n) + \sigma^{\ell}_{pot} \quad \ldots\ldots\ldots(16)$$

The half widths are not fundamental quantities, but may be split up into

$$\Gamma^{\ell}_{a} = T_a \frac{D^a_J}{2\pi} \qquad \Gamma^{\ell'}_{b} = T_b{}^{\ell'} \frac{D^b_J}{2\pi} \quad \ldots\ldots\ldots(17)$$

Where the T are the penetration probabilities. They are defined as

$$T(\alpha) = \frac{\text{number of successful attempts to escape through channel } \alpha}{\text{number of attempts to escape}}$$

where α represents the reaction channels $(a\ell)$ and $(b\ell')$ respectively. In principle these probabilities can be calculated for neutrons and charged particles.

The D's lack such a clear cut definition and cannot yet be computed. They are interpreted, in approximation, as the spacing between the states which can be formed by an incoming particle with a definite angular momentum and spin.

2. Yield of Information.

a) Energy levels.

The energy states of the compound nucleus consist of two groups. The lower group, that of the "bound levels", extends from the ground state to an energy E_{min}, where E_{min} is the smallest of all separation energies E_a of any particle a within the nucleus. The higher group, that of the "virtual levels", extends from E_{min} up, and the emission of particles is possible only for these levels. E_{min} then corresponds to

the ionization energy of an atom, and the virtual levels correspond to the continuum of an atom. By their nature the bound levels therefore can be found only by observing beta or gamma ray transitions, or reactions giving N^{15} as end product, while the virtual levels may be found by observing the resonances of the total neutron cross section and the different reaction cross sections. For the compound nucleus N^{15}, E_{min} is the separation energy of the proton, and its value was reported by Ajzenberg and Lauritzen (1952) to be 10.207 Mev. The separation energy of the neutron is, according to the authors, 10.834, and virtual levels above this energy only can be found by observing resonances in the total neutron cross section. However, since the separation energies of the proton and the neutron are so close, this will cover most of the virtual levels.

b) Angular Momenta.

In the case that the reaction cross sections of the (n,p) and (n,α) reactions are also available, equations (14) and (12) may be used to determine the angular momenta of the different states of the compound nucleus N^{15}. This was done for the lower region (up to E_n = 2 Mev) by Hinchley et al. (1952) and Johnson et al. (1951). Their method may be summarized by the following sequence of operations:

i) Calculate the experimental elastic scattering cross section by subtracting $\sigma(n,p) + \sigma(n,\alpha)$ from σ_t at the different resonances.

ii) Write down the different states that can be formed by neutrons of angular momentum $\ell = 0,1,2,3....$

iii) For these states calculate γ from equation (14), using the experimental values of $\sigma(n,p)$ and $\sigma(n,\alpha)$. Note that there are two values for γ. Which of the two is to be used can be decided only in the next step.

iv) Substitute γ and its appropriate J-value into equation (12) and compare the so obtained $S_J(n,n)$ with the $S(n,n)$ obtained from experimental data in i).

c) Energy Level Spacing, D.

By assigning the angular momentum to a state, the value of γ is also fixed from equation (14). Using, from the total cross section determination, the total width

$$\Gamma^2 = \Gamma_m^2 - \Delta^2 \qquad \text{.....(18)}$$

(where Γ_m is the measured width and Δ the resolution width) Γ_n is found from $\Gamma_n = \gamma\Gamma$, and D_J^n from

$$D_J^n = 2\pi \frac{\Gamma_n}{T_n^\ell}$$

The transmission probabilities may be obtained from

$$T_n = \frac{4xx_o}{x_o^2|v_c|^2 + x^2|v_e^1|^2 + 2xx_o} \qquad \text{.....(19)}$$

where

$$|v_o|^2 = 1$$

$$|v_1|^2 = \frac{(1 + x^2)}{x^2}$$

$$|v_2|^2 = \frac{(9 + 3x^2 + x^4)}{x^4}$$

$$|v_3|^2 = \frac{(225 + 45x^3 + 6x^4 + x^6)}{x^6}$$

$$|v_o^1|^2 = 1$$

$$\left|v_1^1\right|^2 = (1 - x^{-2})^2 + x^{-2}$$

$$\left|v_2^1\right|^2 = (1 - 6x^{-2})^2 + (6x^{-3} - 3x^{-2})^2$$

$$\left|v_3^1\right|^2 = (1 - 21x^{-2} + 45x^{-4})^2 + (45x^{-3} - 6x^{-1})^2$$

$$x = \frac{R}{\lambda\!\!\!^{-}_n}$$

$$x_o = R\left[\frac{1}{\lambda\!\!\!^{-2}_n} + \frac{1}{\lambda\!\!\!^{-2}_o}\right]^{\frac{1}{2}}$$

$\lambda\!\!\!^{-2}_o$ = wave length of neutron inside the nucleus

d.) <u>The Present State of Affairs.</u>

In the region E_n up to 1.8 Mev σ_t as well as σ_α and σ_p have been measured by Hinchley et al. (1952) and by Johnson et al. (1951), and angular momenta have been assigned to most of the states found.

In the region 1.8 to 3.5 Mev all three neutron cross sections have been measured, and energy levels have been assigned by Bollman and Zunti (1951) and by Ricamo and Zunti (1951) but reliable absolute cross section values have been reported only for σ_α. No angular momenta have been assigned.

The region up to E_n = 9 Mev has been investigated by Stetter and Bothe (1951) with continuous neutron energy distribution only. As in this case the outgoing particle energies were measured, the levels may be subject to some uncertainty in the conversion of the number of ion pairs to energy, and for some of the resonances there is the uncertainty that they may lead to an excited state in B^{11}. Furthermore, the Q-values used to compute the neutron energies may induce some additively constant error.

III. DETECTORS

1. General.

For total cross section measurements for fast neutrons the detector is chosen mainly for its ability to distinguish between desirable and undesirable counts. Many of the undesired counts are due to scattered neutrons and can be corrected for in the way described on page 3 by using a monitor. Many of the undesired counts are due to gamma rays. Others are due to neutrons of a different energy, which are produced on or close to the source. Therefore the detector should be, to a certain extent, a proportional counter, i.e. its pulse distribution must be a function of the energy of the incoming neutrons. Furthermore, it should have a low response to gamma rays, since gamma rays will always be present in fast neutron work.

Many different types of fast neutron detectors have been developed which meet these requirements to a reasonable extent. Some of these were developed for applications similar to the one of cross section measurement, i.e. counting all neutrons with energies above a certain bias energy, while others were developed for absolute neutron energy measurements. Since the neutrons themselves do not ionize, all these counters detect neutrons by detection of secondary particles, produced either by collision with neutrons or some form of neutron induced nuclear reaction.

2. "Ideal" Recoil Counters.

Counters in which the secondary particles are produced

by collision are the most common in fast neutron work. Generally, the secondary, or in this case the "recoil", is a proton since neutron proton scattering is isotropic for a large range of neutron energies up to about 10 Mev. Also, the proton recoil energy is larger than that of any other recoil particle, the dependence of the cross section on energy is very well known, and the cross section itself is very large.

The energy of the recoil particle is given by Segre (1953) as

$$E_R = \frac{4M}{(M+1)^2} E_n \cos^2\theta \qquad \text{.....(10)}$$

where M is the mass of the recoil, θ the angle under which the recoil is emitted with respect to the original direction of propagation of the neutron, and E_n is the energy of the incoming neutron. This reduces for protons to the simple form

$$E_R = E_n \cos^2\theta \qquad \text{.....(11)}$$

which gives a maximum recoil energy of $E_R = E$. The maximum energy of the recoil protons will therefore be equal to the energy of the incoming neutrons. The energy distribution of the recoiling protons is uniform from zero to the maximum energy and can be calculated from (14)

$$N(E_R) = \frac{N_o n \sigma}{E_n} \qquad \text{.....(12)}$$

where N_o = number of neutrons between θ and $\theta + d\theta$

n = number of protons per unit area

σ = total cross section for neutron proton scattering.

The yield of hydrogen recoil counters was discussed by Baldinger and Huber (1938), by Barschall and Bethe (1947) and by Rossi and Staub (1949). These authors showed that the distribution in energy of the neutrons may be found relatively

simply from the energy distribution of the recoiling protons, under the condition that the range of the recoils be smaller than the dimensions of the chamber. The measurement of the pulse distribution, however, requires a complicated pulse analyser. But since in the transmission experiment only the number of neutrons above a certain energy is of interest, the gas filled recoil chamber can be used to an advantage by counting only pulses larger than a given size.

If the energy of the smallest recoil pulse counted is B_R, neutrons with an energy $B = B_R$ are the fastest neutrons which still are "biased out". The fraction of recoils above B_R is then

$$\frac{\int_{B}^{\epsilon_m} N(E_R)dE_R}{\int_{0}^{\epsilon_m} N(E_R)dE_R} = \frac{E_n - B}{E_n} = 1 - \frac{B}{E_n} \qquad \text{.....(13)}$$

The total number of recoils produced by neutrons of energy E_m is proportional to the neutron proton scattering cross section, (E_n). The yield is proportional to the fraction of recoils produced, which are of energy greater than B_R, and therefore is proportional to

$$\eta \alpha \sigma(E_n)(1 - \frac{B}{E_n}) \qquad \text{.....(14)}$$

provided the range corresponding to the recoil energy B_R is small compared to the dimensions of the chamber. Making use of the fact that the neutron proton cross section varies approximately as $E^{-\frac{1}{2}}$ for neutron energies above 50 kev, the yield is nearly proportional to

$$\eta \propto E_n^{-\frac{1}{2}}(1 - \frac{B}{E_n}) = B^{-\frac{1}{2}}(x - x^3) \qquad \text{.....(15)}$$

where $x^2 = \frac{B}{E_n}$.

FIG. 2: Yield - Energy Dependance of Hydrogenous Gas Recoil Counters:
(a) "Ideal Counter"; (b) $\frac{R_o}{a} = 0.5$; $\frac{R_o}{b} = 4$;
(c) $\frac{R_o}{a} = 0.9$, $\frac{R_o}{b} = 7.2$.

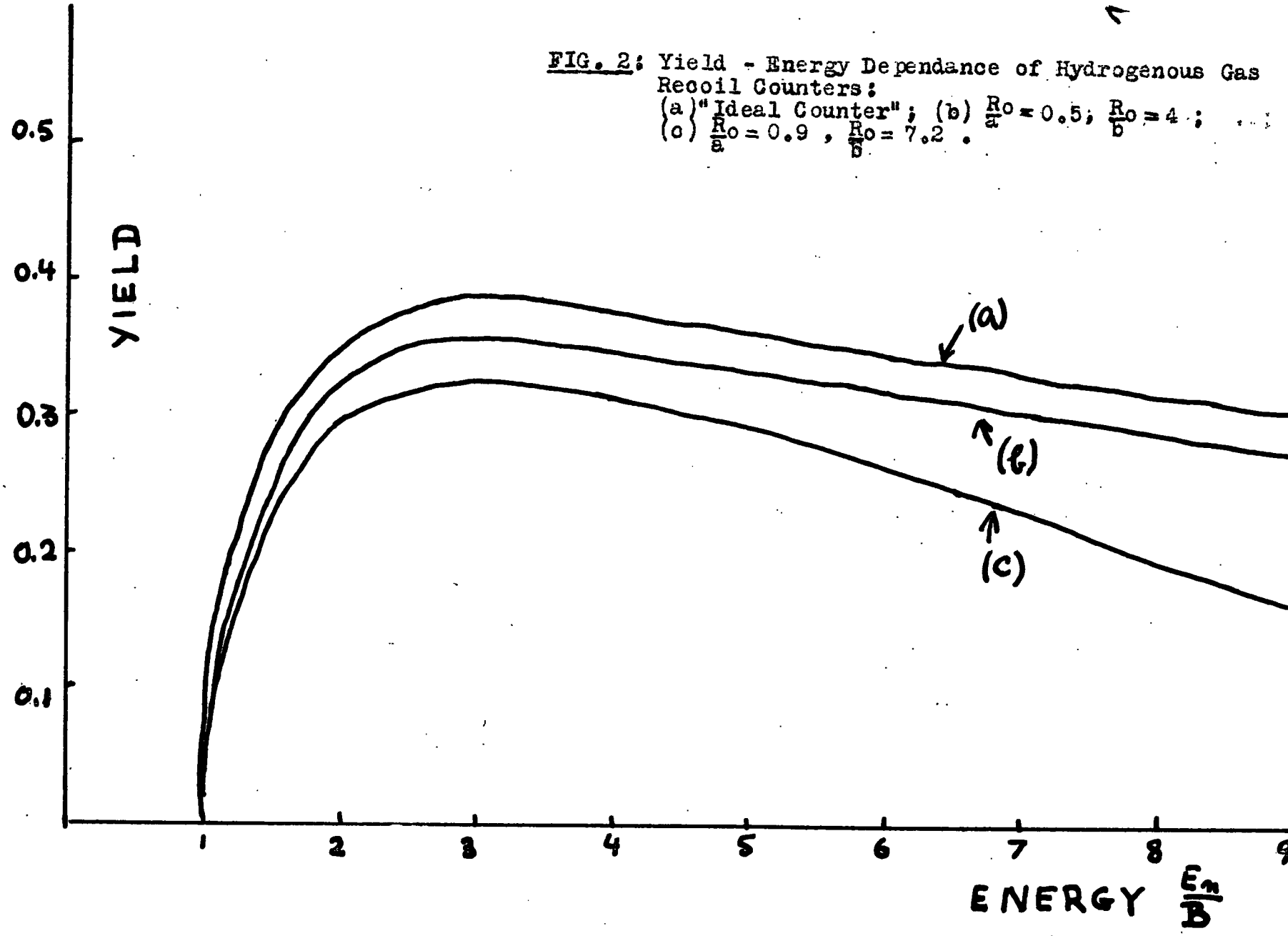

To follow page 15

Rossi and Staub (1949) showed that if

$$\sigma_s(E) = \sigma_o E_n^{-\frac{1}{2}} \qquad \ldots\ldots\ldots(16)$$

is the cross section of hydrogen, then the constant of proportionality is given by

$$\epsilon_B = t\nu\sigma_o B^{-\frac{1}{2}} \qquad \ldots\ldots\ldots(17)$$

where ϵ represents the efficiency of the radiator for neutrons of energy E = B; t is the thickness of the radiator in micrograms per cm^2, and ν the number of hydrogen atoms per microgram. In general, according to these authors, the yield will then be given by

$$\eta = \epsilon(E_n)\, F\left(\frac{B}{E}\right) \qquad \ldots\ldots\ldots(18)$$

where $(E_n) = t\nu\sigma_s(E_n)$ is the efficiency of the radiator and F is the integral pulse height distribution, as can be seen from Fig. 2a. The function $x - x^3$ has a minimum at $x^2 = \frac{1}{3}$ or E = 3B. It does not vary more than 25% from its maximum value in the energy interval

$$1.57\ B < E_n < 9.6B \qquad \ldots\ldots\ldots(10)$$

As can be seen on Fig. 2a the yield of the counter as a function of energy rises sharply and remains constant for a wide range of neutron energies. There is, therefore, a threshhold detector of particularly desirable features, in contrast to the reaction counters, whose yield varies in an arbitrary manner above the threshhold. For a certain bias, B, the number of counts observed is roughly proportional to the number of neutrons with energies greater than approximately 1.5B. This convenient relation is due to the simple dependence of the hydrogen cross section on energy.

3. Recoil Gas Counters.

Although for use as threshhold detector the exact knowledge of the expected pulse height distribution of a counter is of no direct interest, it provides the only really good check upon whether the counter is behaving properly. In an ideal counter all recoils would be produced and stopped inside the sensitive volume. In the transmission experiment however, a compromise must be found between good geometry and counter behaviour, and the counter diameter will therefore have to be kept small. Also because guard rings have to be placed around the ends of the wire in order to have a well defined sensitive volume, some recoils will always be produced outside the sensitive volume; and there will always be some neutrons which penetrate sufficiently far into the sensitive volume to produce recoils that leave the volume.

Rossi and Staub (1949) calculated the differential and integral pulse height distributions taking into consideration the fact that the counter diameter is smaller than the range of the recoils (wall effect) and the fact that not all recoils are produced or stopped in the sensitive volume (end effect). These distributions are given as function of pulse height, P (in mev), divided by the energy of the incoming neutrons, E_n. The differential distribution is

$$f\left(\frac{P}{E_n}\right) = 1 + \frac{R_o}{a} L \left(\frac{P}{E_n}\right) + \frac{R_o^2}{ab} M \left(\frac{P}{E_n}\right) + \frac{R_o}{b} N \left(\frac{P}{E_n}\right) \quad \ldots\ldots(19)$$

and the integral distribution

$$F\left(\frac{P}{E_n}\right) = \left(1 - \frac{P}{E_n}\right) + \frac{R_o}{Q} Q \left(\frac{P}{E_n}\right) + \frac{R_o^2}{ab} S \left(\frac{P}{E_n}\right) + \frac{R_o}{b} T \left(\frac{P}{E_n}\right) \quad \ldots(20)$$

The distributions apply only if the maximum range, R_o, of the recoils is smaller than the length "a" of the counter. "b" is the diameter of the counter. The functions L, M, N, Q, S and T were calculated by Rossi and Staub (1949) and may be found in their book tabulated for values of $\frac{P}{E_n}$ from zero to one.

Skyrme, Tunnicliffe and Ward (1952) also calculated the differential pulse height distribution, considering wall and end effects. They obtained the following formula

$$f(x) = 1 + \frac{R_o}{b}\frac{dI_1}{dx} + \frac{R_o}{Q}\frac{dI_2}{dx} - \frac{R_o^2}{ab}\frac{dI_3}{dx} \quad \ldots\ldots(21)$$

where $x = \frac{P}{E_n}$. However, this distribution applies only if the range of the recoil is smaller than the length and the diameter of the sensitive volume. These conditions can hardly be met in a transmission experiment with fast neutrons, while Rossi and Staub's conditions are easier to satisfy, since a small counter diameter is permitted. The functions I_1, I_2 and I_3 and their derivatives were calculated by Skyrme, Tunnicliffe and Ward (1952) and are tabulated in their paper for values of x from zero to one and neutron energies of 0.25, 0.50 and 1 Mev.

In order to estimate the influence of the wall and end effects on gas counter in use as threshhold counters, the yield as a function of energy was calculated from equation (18), using Rossi and Staub's (1949) integral pulse height distribution (equation 20) and their tables for the functions Q, S and T. The range was assumed to be proportional to E. Fig. 2b shows the yield for a counter of such dimensions that $\frac{R_o}{a} = \frac{1}{2}$ and $\frac{R_o}{b} = 4$, for a neutron energy of E = 5B. For Fig. 2c the

dimensions are $\frac{R_o}{a} = 0.9$ and $\frac{R_o}{b} = 7.2$ for E = 5B. Fig. 2a was already mentioned above, as representing an "ideal" counter, i.e. $\frac{R_o}{a} = 0$ and $\frac{R_o}{b} = 0$. Thus when the maximum range of the recoils becomes close to the counter length (case c), there is a large reduction in yield at the higher energies, which is presumably due to the end effects. This causes the straight part of the curve to be steeper, and the energy dependence of the yield will, therefore, be greater. With a counter length which is twice the range (case b), there is no such decrease in yield for high energies, the shape of the curve being practically the same as for the "ideal" counter. The reduction in yield is distributed evenly and is presumably mainly due to wall effect. Thus the size of the diameter, which is the important component in counter design for transmission experiments, does not considerably affect the shape of the response, but only the overall yield. On the other hand, the length of the counter, which has little bearing on the transmission experiment, affects considerably the shape of the response.

4. Counters using Solid Radiators.

While in the above discussions it was assumed that the recoils are produced by the gas filling of the counter, the recoils may also be produced by a solid hydrogenous "radiator" mounted close to or inside the counter. In such a case "ideal" counter behaviour can be obtained only with infinitely thin radiators. These are impractical since the efficiency is proportional to the thickness of the radiator. Finite radiator thicknesses will give a reasonably practical yield, while still

preserving the flatness of the "ideal" yield-energy response, or even improving it.

The differential and integral pulse height distributions for solid radiator counters were calculated by Rossi and Staub (1949). The integral distribution is given by

$$F\left(\frac{P}{E}\right) = \int_{P/E_m}^{1} \frac{1}{t} X \left(\frac{E}{E_n}, \frac{P}{E_n}\right) d\left(\frac{E}{E_2}\right) \qquad \text{.....(22)}$$

where $$X = R_o^1 \left[\left(\frac{E}{E_n}\right)^{3/2} - \left(\frac{P}{E_n}\right)^{3/2} \right]^2 \quad \text{when } X < t$$

and $$X = t \quad \text{otherwise.}$$

If $R'(E)$ is the range in the material of the radiator then R'_o is assumed to be $R'(E) = R'_o E^{3/2}$. The integration of equation (22) was performed by these authors, and the results are shown in the form of graphs in their book for different values of $\frac{t_o}{R'_o} < 1$. The differential distributions are also shown, as calculated by these authors by differentiating the integral distributions. For $\frac{t}{R'_o} \geq 1$ there is always $x \leq t$, and $F\left(\frac{P}{E_n}\right)$ may readily be integrated

$$F\left(\frac{P}{E_n}\right) = \frac{R'_o}{t}\left[1 - \left(\frac{P}{E_n}\right)\right] \qquad \text{.....(23)}$$

From equation (18) then the yield for "thick" radiators will be

$$\eta = \frac{1}{3} \zeta_B \frac{E_n}{B} \left[1 - \left(\frac{B}{E_n}\right)^{3/2}\right]^2 \qquad \text{.....(24)}$$

if R' is assumed to be proportional to $E^{3/2}$. The factor ζ_B is given by

$$\zeta_B = R'(B) \nu \sigma_o B^{-1/2} \qquad \text{.....(25)}$$

and represents the average number of recoils per incident neutron of energy $E_n = B$.

Since equation (22) as it stands, does not give any direct information on the dependence on the range of the integral

To follow page 20

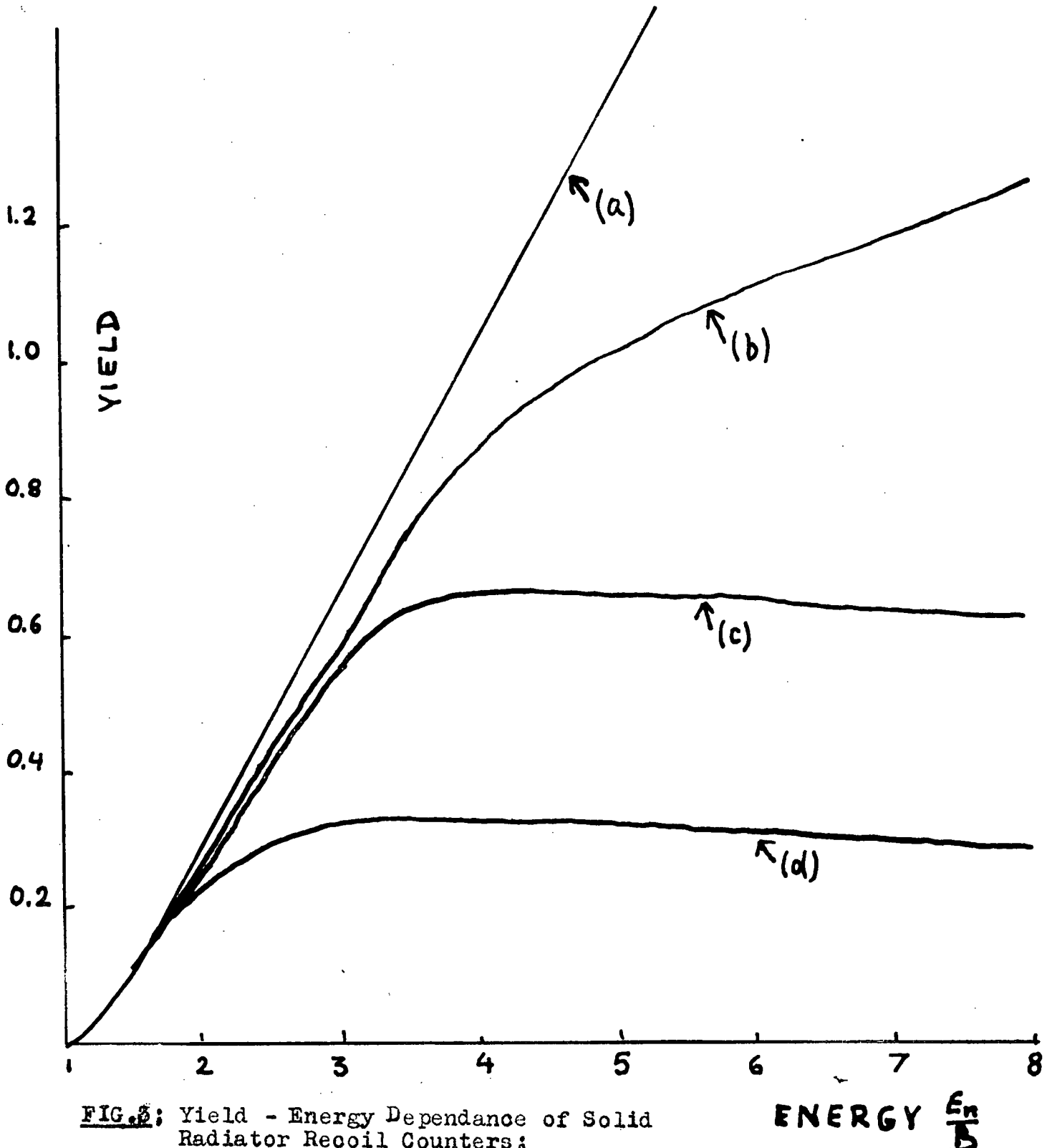

FIG.2; Yield - Energy Dependance of Solid Radiator Recoil Counters; (a) Thick Radiator; (b) $\frac{t}{R_o}$ 0.75; (c) $\frac{t}{R_o}$ 0.25; (d) $\frac{t}{R_o}$ 0.10 .

distribution, the yield for "thin" radiators was estimated the following way. From Rossi and Staub's curves of the integral distributions as functions of $\frac{P}{E_n}$ curves were plotted for $F(\frac{P}{E_n})$ as a function of $\frac{t_o}{R_o}$ for different values of $\frac{P}{E_n}$. Then, assigning nominal thicknesses of $\frac{t_o}{R_o} = 0.1$; 0.25; and 0.75; to the point $E_n = B_1$ the effective thicknesses were calculated for different neutron energies $\frac{E_n}{B}$ from one to 10, assuming the range to be proportional to $E_n^{3/2}$. Using these values, $F(\frac{B}{E_n})$ could be read off the curves of $F(\frac{P}{E_n})$ vs. $\frac{t_o}{R_o}$ for each desired neutron energy. Thus, values for $F(\frac{B}{E_n})$ as a function of neutron energy were obtained for three different nominal thicknesses. Inserting these into equation (18) the yield as a function of neutron energy was obtained for three different radiator thicknesses. These are graphically represented on Fig. 3b, c, and d. Fig. 3a represents the yield of a thick radiator, calculated from equation (23). As in equation (23) the yield is independent of the radiator thickness, the one curve will demonstrate the behaviour of all thick radiators.

Fig. 3 illustrates the continuous transition of the energy response of solid radiator counters from the thin to the thick case. Curves d and c show close resemblance to the ideal curve, and due to the increase of the yield with radiator thickness, they indicate even less energy dependence than that of the ideal counter. As the radiator becomes thicker, however, the response approaches more that of a thick radiator, and the energy dependence of the yield increases. The overall yield increases

with the thickness of the thin radiator. Thus there is low yield in the region of flat response and high yield in the region of steep response. It must be noted, however, that these considerations are made for counters with no wall and end effects. Since these effects tend to decrease the yield more for the higher energies, it might be possible, by proper choice of counter dimensions, to obtain flatter response for thicker radiators and therefore for higher yields.

5. Practical Considerations.

In the transmission experiment, as in most experiments, high counter yield makes it possible to obtain better statistics in shorter time. Since, in order to obtain a good energy resolution, it must be tried to keep the target as thin as humanly possible, since it must be tried to keep the points of measurement as close as possible, and since the elimination of background requires three measurements for each point, the experiment will tend to be rather lengthy. It is therefore specially desirable to raise the counter yield as much as possible. Equation (17) shows that this can be done by keeping the bias energy as low as background and parasitic components will permit. For gas counters the yield can be improved further by increasing the factor t by increasing the gas pressure, and using a gas of high hydrogen content, like a heavy hydrocarbon. This will at the same time reduce the range and consequently the wall and end effects, and therefore will result in a better response. For solid radiator counters the yield could be improved by increasing the radiator thickness, but only at the expense of the flatness

of the response.

Although in this type of experiment the results are independent of the absolute yield of each of the two counters, the ratio of the yields of the two counters must stay constant during the whole time of measurement for each point. Flat yield to energy response is therefore an important characteristic, since otherwise an involuntary change in bias, or supply voltage, would change the counting rate of one counter with respect to the other. One could try to reduce this danger by increasing the yield and therefore reducing the counting time. But generally a system will have nearly the same stability over five minutes as over half an hour, and it is therefore to be preferred not to sacrifice flatness in response for shorter counting time.

On the other hand it would be unwise to try to achieve optimum response by means of complicated construction of the counter. A well defined and preferably round counting area is important as it simplifies the estimation of geometrical effects. The area should be small, but will have to be a compromise between yield, response and geometrical considerations. Generally it will be found that simplicity in construction is easier obtained with a gas counter than having a solid radiator. Since the depth of the counting volume does not affect the geometrical corrections the counter should be made sufficiently long to make end effects negligible. This at the same time gives the counter a more directional response, and therefore helps to reduce the background counting rate.

6. Recoil Scintillation Counters.

While gamma ray scintillation counters have made rapid advances in recent years and are widely used, neutron scintillation counters are still in the early development stage. Although the experience gained in photomultiplier and electronic techniques is certainly of great help to the development of neutron counter, the development of scintillators for neutrons has to go on a completely independent line, because in most fast neutron work a high gamma ray sensitivity of the counter is undesirable.

Most of the considerations of the previous sections will apply equally to recoil scintillation counters. If the scintillator and the radiator are either the same substance, or form an isotropic mixture, one should expect a counter behaviour similar to that of a hydrogenous gas counter. If the scintillator and the radiator lie in different layers one should expect behaviour similar to that of solid radiator counters. Matters can become by far more complicated, however, if the light output of the arrangement is not proportional to the energy of the recoil protons. Unfortunately, in many practical cases this will occur.

Anthracene as a scintillator for neutron counting has been used since 1947 (Collins, 1948; Moon, 1948; Deutsch; Marshall and Coltman, 1947; Mallman, 1947; Huber et al. 1949). Its high light output, short pulses, and high proton content make it appear most suitable. Since the pulse height is nearly proportional to the recoil energy (Krebs, 1953), and

since, due to the high stopping power of anthracene, one can avoid practically all wall and end effects, the response of anthracene counters should be very similar to that of "ideal" gas counters. However, in spite of all these favorable features anthracene counters are unsuitable for most fast neutron work because of their extremely high gamma ray sensitivity. Similarly several organic solutions which have been investigated by Keeping and Lovberg (1952) for application as neutron scintillators show too high a gamma ray sensitivity to be practical. Furthermore, insufficient information on the energy response of such solutions is available, so that their suitability for threshhold counters cannot be predicted.

In contrast to the organic scintillators, zinc sulfide shows extremely low sensitivity for gamma rays. Consequently the more recent investigations for heavy particle detection concentrate more on this scintillator. Because ZnS is an opaque powder its light output increases with scintillator thickness only to a certain point. Its output then decreases with further increase in thickness, as the light absorption of the scintillator becomes comparable to the output. The pulse height distribution for ZnS recoil counters consequently will be completely different from the recoil energy distribution and it will be difficult to predict the response of such a counter.

The simplest case to consider would be that of an isotropic mixture of zinc sulfide with a transparent hydrogenous material. Here, as a rough guess, pulses can be expected only from those recoils that were formed so close to the photocathode

that not all the light which was originated by them could be absorbed. This should result in a response similar to that of the thick solid radiator, where only those recoils can be counted which are formed so close to the edge as to be able to leave the radiator. One could therefore expect to obtain similar response for these two cases. Hornyak (1952) developed such a counter by molding ZnS powder uniformly into Lucite. His yield energy response is very similar to that of thick solid radiators. For a fixed bias the yield increases nearly linearly with the neutron energy. While such a response is not very suitable for transmission experiments the counter shows otherwise very desirable features. The counting volume can easily be adapted to the needs of the experiment. The yield is very high (up to 8%), and over a wide range of ZnS densities it does not vary with weight of ZnS per gram of Lucite, so that it should be relatively easy to construct counter and monitor with the same characteristics. Gamma counts are so low that 17 mev gammas can be completely biased out when counting 0.5 mev neutrons, without having to sacrifice a considerable amount of the yield.

For the case that the radiator and the Zinc sulfide are in two separate layers the situation is more complicated. For monoenergetic neutrons the recoils leave the radiator at different angles, and therefore effectively encounter different scintillator thicknesses. In addition, at each angle there are recoils of various energies, depending on the depth of their point of origin in the radiator. Thus the pulse distribution of such counters will be determined by the

dependence of the light output of ZnS on the neutron energy and the thickness of the ZnS layer as well as by the recoil energy distribution. However, for very thin radiators combined with thin layers of ZnS, one might expect these effects to be relatively small, and it might be possible to obtain a counter behaviour similar to that of thin solid radiator counters. Several methods have been developed to provide uniform ZnS screens for alpha particle and proton detection (Caldwell and Armstrong, 1952; Graves et al. 1952). In one of these, the screen is mounted on Lucite backing and therefore should be practical for neutron counting. The others probably could be easily adapted for neutron counting by adding a hydrogenous radiator, e.g. paraffin or Lucite. Unless the scintillator and the radiator are kept relatively thin, however, it is difficult to determine the type of response which may be expected from such counters.

7. Neutron Reaction Counters.

Although recoil counters are predominantly employed in fast neutron work, counters producing secondary particles by means of a nuclear reaction have been tried; it was found that they have a few advantages over the recoil method. It seems, however, that these advantages are outweighed by one great disadvantage, namely the irregularity of the yield energy response.

The main advantage of the reaction counter is that its pulse height is proportional to the energy of the incoming neutron. This means that the number of pulses of size P will

To follow page 27

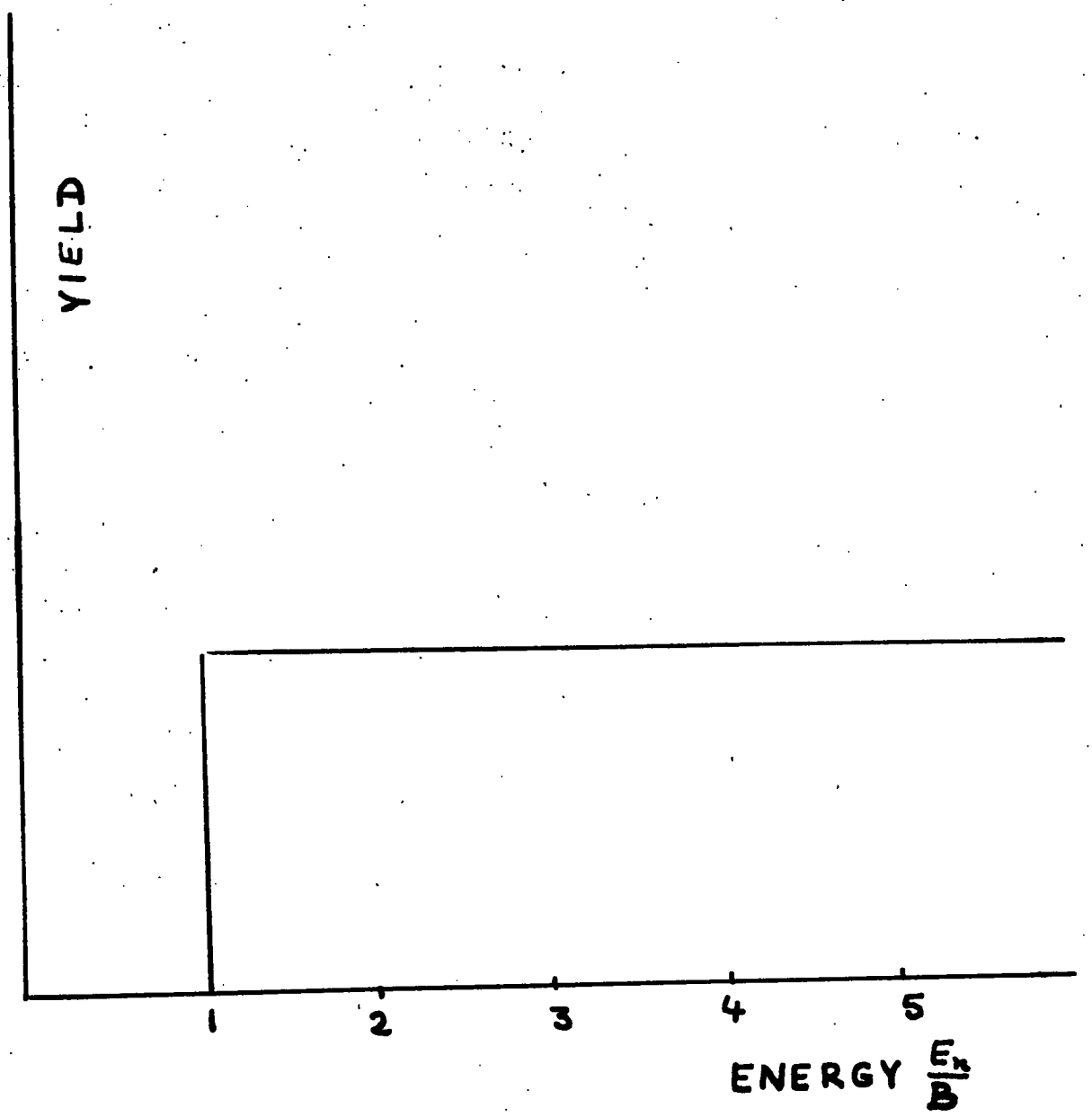

FIG. 4 : Yield - Energy Dependance of an Ideal Reaction Neutron Counter.

be given by

$$N(P) \propto N_o(E_n)\,\sigma(E_n) \qquad \ldots\ldots\ldots(26)$$

where $N_o(E_n)$ is the number of neutrons of energy E_n and $\sigma(E_n)$ is the total reaction cross section. If we could find a reaction which had a cross section which is independent of the neutron energy we would have the perfect threshhold detector, the yield energy response for fixed bias being as shown on Fig. 4. In practice, the response will take the shape of the variations of the reaction cross section with energy.

The following reactions are most commonly tried for neutron reaction counters:

$$Li^6 + n \rightarrow He^4 + H^3$$
$$B^{10} + n \rightarrow Li^7 + \alpha$$
$$N^{14} + n \rightarrow C^{14} + p$$
$$\rightarrow B^{11} + \alpha$$

Of these the $B^{10}(n\alpha)$ reaction is used much more than any of the others. It has a very large cross section and is also known to obey the $\frac{1}{v}$ law in the low energy region, ($E_n < 500$ ev.). It therefore provides a very suitable counter for thermal neutrons or for flux measurements where no bias is required; since then the neutrons can be slowed down to thermal velocities before entering the chamber. For higher energies all the above reactions are reported to have resonances. Furthermore the complication enters that the material used has to be employed generally as some chemical compound, and therefore it must be counted with possible resonances in the other nuclei that are present.

As mentioned, the boron reaction is the most commonly

used, the boron being chiefly in the fluoride form. The applicability of such counters for fast neutron work was studied by James (1953), and by James et al. (1955), by investigating the pulse height distributions at different neutron energies of two BF_3 counters of different isotopic content of B^{10}. The results showed several resonances, most of which were assigned to B^{10} reactions. The conclusion was reached that BF_3 gas is not suitable for neutron spectroscopy. For use as a threshhold detector in transmission experiments the BF_3 counter is unsuitable, since there a simple dependence of the yield on energy is desired.

At the University of British Columbia, Flack and Warren investigated the $Ne^{20}(n,\alpha)O^{16}$ reaction, which yields a single α-group up to neutron energies of approximately 3 Mev, and only two α-groups for neutron energies from 3 to 5.5 Mev. The cross section, while adequte, fluctuates rather more than desirable for a fast neutron counter.

The introduction of neutron reaction scintillation counters so far has not solved this problem. Although already several different counters, and many different scintillating materials, have been tried (Schenck, 1952), they all concentrate around the Boron and the Lithium reaction, and are specifically designed for slow neutron work. No indication can be obtained from these investigations as to whether such counters would be suitable for fast neutron work.

IV. NEUTRON SOURCES

In recent years the interest in cross section measurements has been concentrated as much on the variation of the cross section with energy, as on its actual value. If the transmission experiment is to be employed a source of monokinetic neutrons is therefore needed, and this source must be capable of delivering monokinetic neutrons over a whole range of energies. The energy spread of such a source then will determine the energy resolution of the experiment. Since it generally will be attempted to find resonances in the energy dependence of the cross section, the energy resolution should be smaller than the width of these resonances. Natural sources have much too wide an energy spread to be suitable, and electrostatic generators will therefore usually be employed in investigations with neutron energies of a few Mev.

Since, when planning a particular experiment, generally the properties of the particle accelerator cannot be chosen, the efforts in obtaining an optimum source will have to be concentrated on the target. The problem of choice of the target is extensively discussed by Graves et al. (1952). The target reactions which are, according to these authors, the most important, are listed below in Table I. Along with the reactions and their Q-values, the neutron energies obtainable from these reactions with an accelerator capable of 1.5 Mev are listed. This indicates that, except for energies below 1 Mev, there is one reaction common for each neutron energy

Table I

Reactions employed commonly in the production of neutrons

Reaction	Q-value	Approx. En. with 1.5 Mev Accelerator
$C^{12} + d \rightarrow N^{13} + n$	- 0.26	0 to 1 Mev
$T^{3} + p \rightarrow He^{3} + n$	- 0.76	0 to 1
$Li^{7} + p \rightarrow Be^{7} + n$	- 1.65	-
$D^{2} + d \rightarrow He^{3} + n$	+ 3.28	2 to 5
$N^{14} + d \rightarrow O^{15} + n$	+ 5.1	5 to 7
$T^{3} + d \rightarrow He^{4} + n$	+17.6	13 to 18

region, and consequently the target reaction will be generally chosen by its neutron energy region rather than by other considerations. Many accelerators, however, may give higher potentials, and the neutron energy regions of the reactions then may overlap.

As mentioned in the Introduction, the energy region of N^{15} which was to be investigated, is the one that corresponds to neutron energies above 3.5 Mev, and the D(d,n) reaction was chosen for neutron production. This reaction was investigated by many workers for neutron energies up to 4 Mev.

The angular distribution of the neutrons was found by Humber and Richards (1949) to be $A + B\cos^2\theta + C\cos^4\theta + D\cos^6\theta$ but the much simpler distribution of $A + B\cos^2\theta$ is reported by Graves et al. (1952) to be correct for deutron energies up to approximately 1 Mev. The neutron yield will thus be greatest in the forward direction. For deutron energies below 400 kev, thick targets produce 2.5 Mevmonoenergetic neutrons at an angle

of 90°, while in the forward direction the neutrons will take the spectral distribution of the neutron beam. These energies however, will be weghed towards the higher values, because the yield increases rapidly with the energy.

For deuteron energies above 500 kev monochromatic neutrons can be obtained with thin targets only. Such targets are often gas volumes which are seperated from the accelerator tube by an aluminum foil. These targets may present considerable difficulties because of large background produced by such foils. While it is easier to obtain aluminum foil that that produces small energy losses, nickel foils give less background. Deuterium ice targets are also employed. Since the heavy ice can be deposited in such a way that it faces the beam directly, there will be no stopping of the deuterium beam, and therefore no thin foils to worry about. For both gas and ice targets there may be considerable neutron background due to deuterons interacting with carbon deposited in the target area and on the target itself. This carbon originates from oil vapour in the vacuum system, and can be considerably reduced by using liquid air traps. Another serious source of background may be the contamination of deuterium in the target area and on the target. Neutrons due to contamination in the target area will have different angles and therefore different energies, and contamination will take place mostly at the beam defining apertures; it can be reduced by heating these apertures. Contamination in the target support will result in lower energy neutrons, since the beam has to

pass the target and part of the target support before reaching this deuterium. Background due to such contamination can be considerably reduced by changing the target support frequently.

To follow page 33

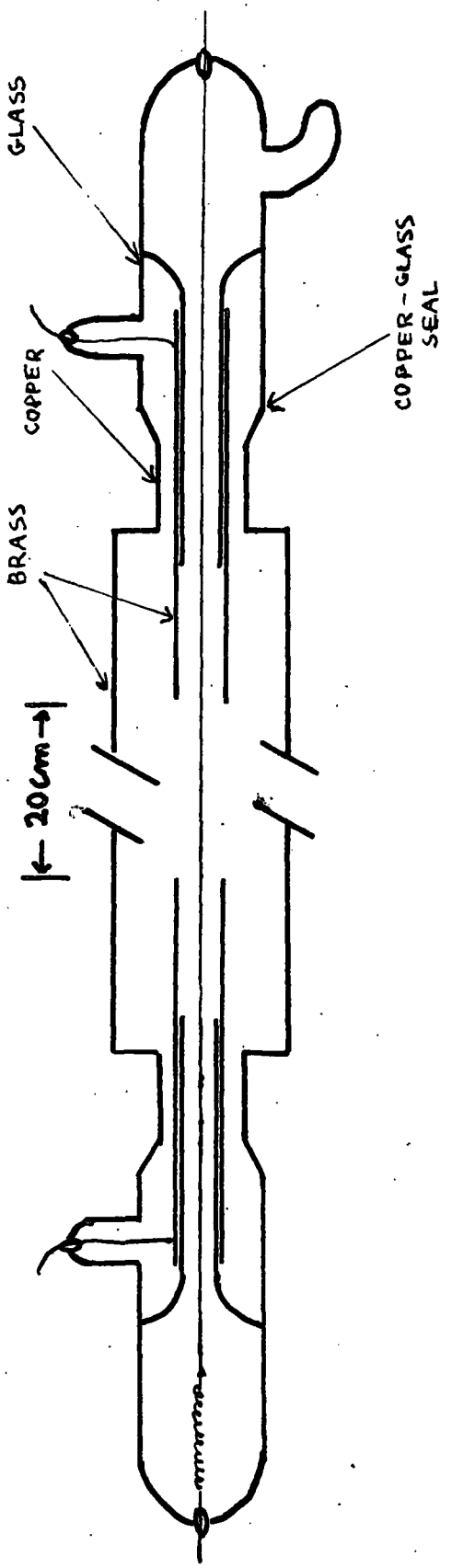

FIG. 5: The Propane Counters.

V. EXPERIMENTAL ARRANGEMENT

1. Counters.

As was pointed out in chapter I, two counters, preferably of similar behaviour, are necessary for the transmission experiment. It was thus decided to construct two propane proportional counters as illustrated in Fig. 5. The choice fell on a gas radiator counter because it was felt that in accordance with the discussions of chapter III this type would combine simplicity of construction with good response, even when considerable wall effects are present. Propane was chosen rather than methane or hydrogen, because propane has a higher hydrogen content and a higher stopping power. Furthermore, the relatively high boiling point of propane ($-42^{o}C$) simplified considerably the purification of the gas.

Fig. 2 in chapter III indicates that for a proton range R_o, and counter length $2R_o$ and diameter $\frac{1}{4}R_o$ it may be expected that the wall and end effects still may permit a reasonably good yield energy response. Thus, in order to decide on the dimensions of the counter, the range of 4 Mev protons in propane (C_3H_8) was calculated with the help of the curves of proton ranges in air, and of the relative stopping power, which were published by Livingston and Bethe (1937). The range, according to these authors, is given by

$$\text{Range in propane} = \frac{\text{Range in Air}}{\text{St. Power Rel.to Air of propane}} \qquad \ldots\ldots\ldots(27)$$

The range of 4 Mev protons in air was read from the curves as

To follow page 34

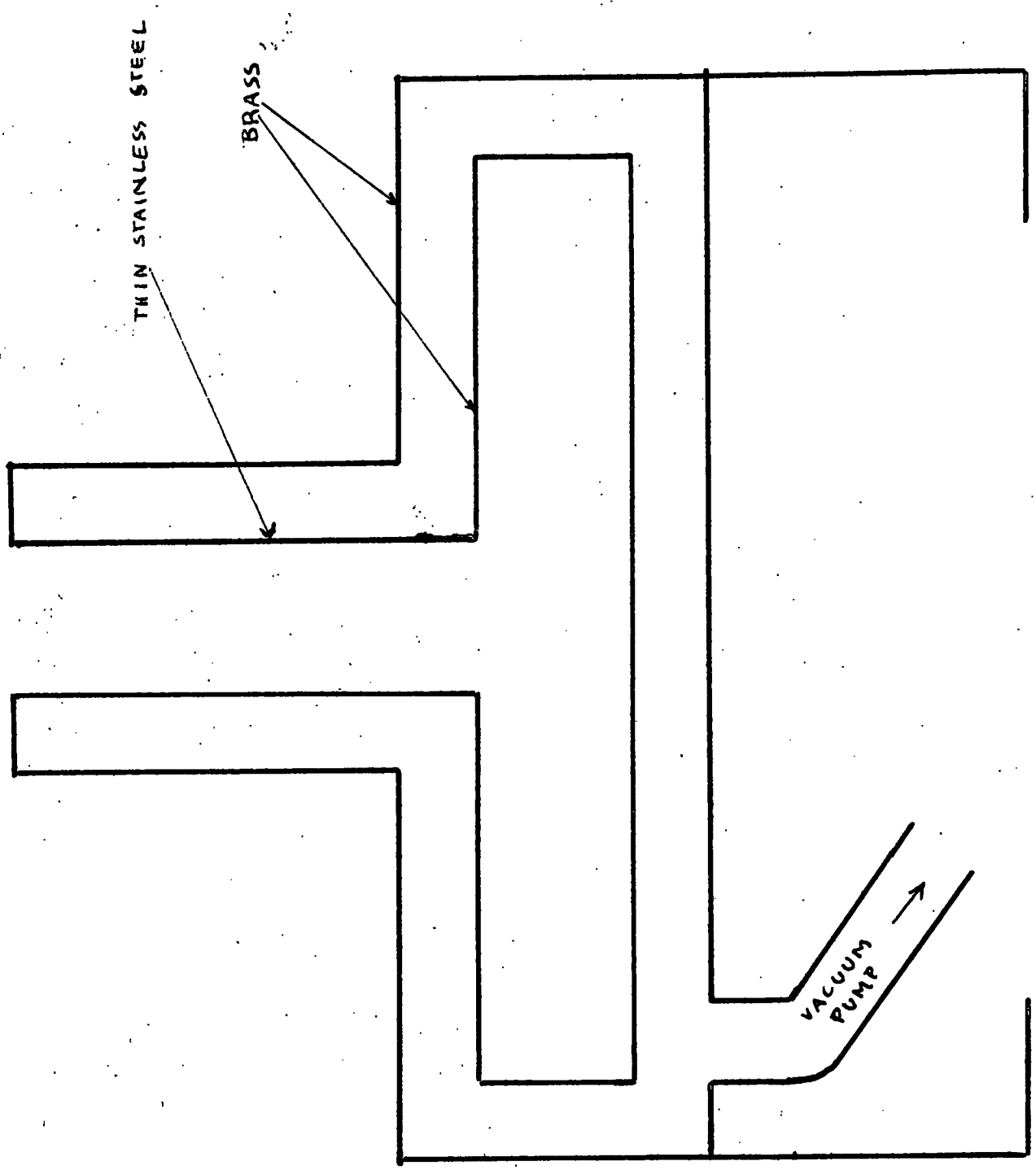

FIG. 6: The Nitrogen Containers.

R_a = 23.1 cm. The relative stopping power of carbon was read as 0.911 and that of hydrogen as 0.197; that of propane thus was calculated to be

$$(\text{St. Pwr})C_3H_8 = \frac{3}{2} \times 0.911 + 4 \times 0.197 = 2.15$$

and the range of 4 Mev protons in propane will be

$$R_o = \frac{23.1}{2.15} = 10.7 \text{ cm}$$

Consequently the counter length was chosen 20 cm, and a diameter of 1" was estimated to be suitable with respect to counter behaviour as well as with respect to geometry (c.f. section 4 of this chapter).

The thickness of the tungsten wire anode was chosen 3 thou in accordance with recommendations by Korff (1947) and by other workers in this laboratory. The length of the extension of the counter beyond the sensitive volume, the diameter of the guard rings etc. were mainly determined by practical considerations, such as the kind of copper glass seals, glass and brass tubing available etc.

The pulse height distribution to be expected from these counters was calculated from equation (19) and is shown in Fig. 6. The calculation of the yield energy response has already been discussed and illustrated above (chapter III and Fig. 2). The counting yield can be calculated from equations (18) and (17).

$$\eta = \varepsilon_B \left(\frac{E_n}{B}\right)^{-\frac{1}{2}} F\left(\frac{E}{B}\right) \qquad \text{.....(18)}$$

$$\varepsilon_B = t\nu\sigma_0 B^{-\frac{1}{2}} \qquad \text{.....(17)}$$

Assuming a bias energy of 0.5 Mev, for 4 Mev neutrons

the relative neutron energy will be $\frac{E_n}{B} = 8$, and therefore, according to Fig. 2 the ratio of yield over radiator efficiency may be expected to be $\frac{\eta}{\varepsilon_B} = 0.3$. The number of hydrogen atoms per cm^2, $t\nu$, will be equal to the number of hydrogen atoms in 20 cm^3 propane (C_3H_8)

$$t\nu = (8)(20)\frac{A}{Vm}\frac{p}{76} = \frac{(8)(20)(6)(10^{23})}{(2.24)(10^3)}\frac{p}{76} = (3.5)10^{21}\frac{p}{76}$$

where A is Avogadro's number, Vm is the volume of one mole at atmospheric pressure, and p is the filling pressure of the counter in cm Hg.

σ_o was assumed to be 4.2 barn, using the relation $\sigma = \sigma_o E^{-\frac{1}{2}}$ to calculate it from cross section values for neutron proton scattering published by Adair. This gives a radiator efficiency of

$$\varepsilon_B = \frac{(3.5)(10^{21})(4.2)(10^{-24})}{0.5} = 2.1\%\ \frac{p}{76}$$

and a counter yield

$$\eta = 0.3\varepsilon_B = 0.63\%\ \frac{p}{76}$$

The counters were thoroughly cleaned with nitric acid, acetone and alcohol, and outgassed while heated at 0.1 micron pressure. This was done for two days, until it was found that no increase in pressure occurred in the counters, when they were left closed up for twelve hours. Although it was stated by the manufacturers to be chemically pure, the propane used for the filling of the counters was condensed in a dry ice alcohol trap in the vacuum system. This procedure made it possible to evaporate only part of the propane, so that it can be assumed that no heavier hydrocarbons were present. Furthermore, all air that could have entered the system together with the propane

could be pumped out completely before filling. The pressure was chosen 54.1 cm Hg, which is sufficiently below atmospheric to enable the glass-blower to seal off the glass seals. This pressure, according to the calculation of above, would give a counter yield of 0.45%.

2. Absorbers.

As was discussed in chapter I, best accuracy of the cross section measurements may be obtained when three measurements are taken for each neutron energy: one without absorber, one with a known absorber and one with the unknown absorber. Furthermore it was argued that it is of advantage to use the absorbers in liquid form. It was therefore decided to take water as known absorber because of its low transmission, and three brass Dewars were constructed as illustrated in Fig. 6. Since by using metal containers it is easier to make containers of the same shape, it was felt it would be of advantage to have three containers rather than one. This would avoid time delay, and contamination of the nitrogen, due to refilling with a different absorber between each measurement.

It was decided to base the choice of the length of the containers on a transmission of approximately 0.5, because different writers do not seem to agree whether it is better to choose a transmission above or below this value. Furthermore it was felt, since the cross section of N^{14} had to be estimated, this was the best way to ensure that the actual transmission would be neither too large nor too small. Thus, using a transmission of 0.5, the desired length of the absorbers was

To follow page 37

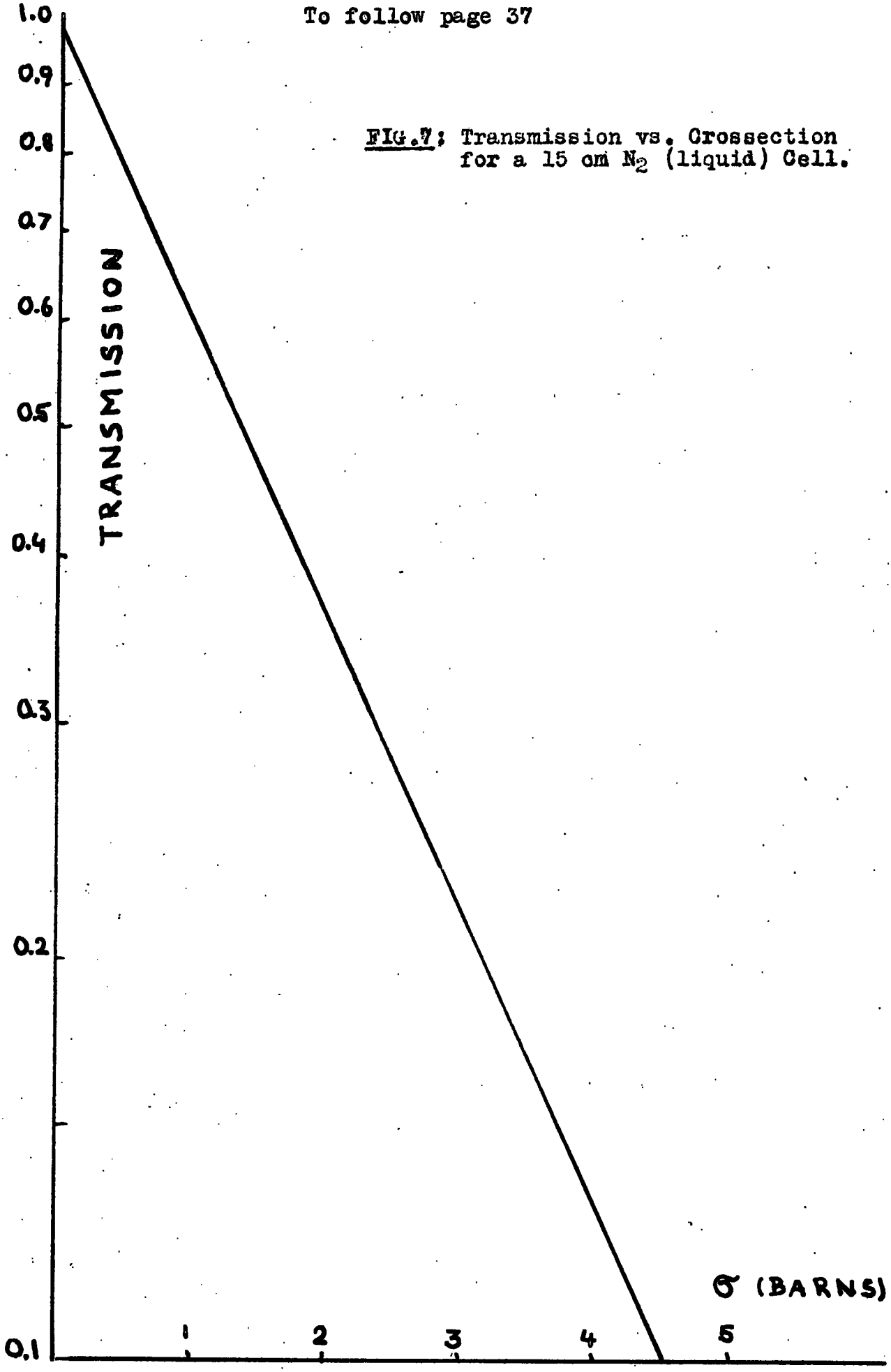

FIG.7: Transmission vs. Crossection for a 15 cm N_2 (liquid) Cell.

To follow page 37

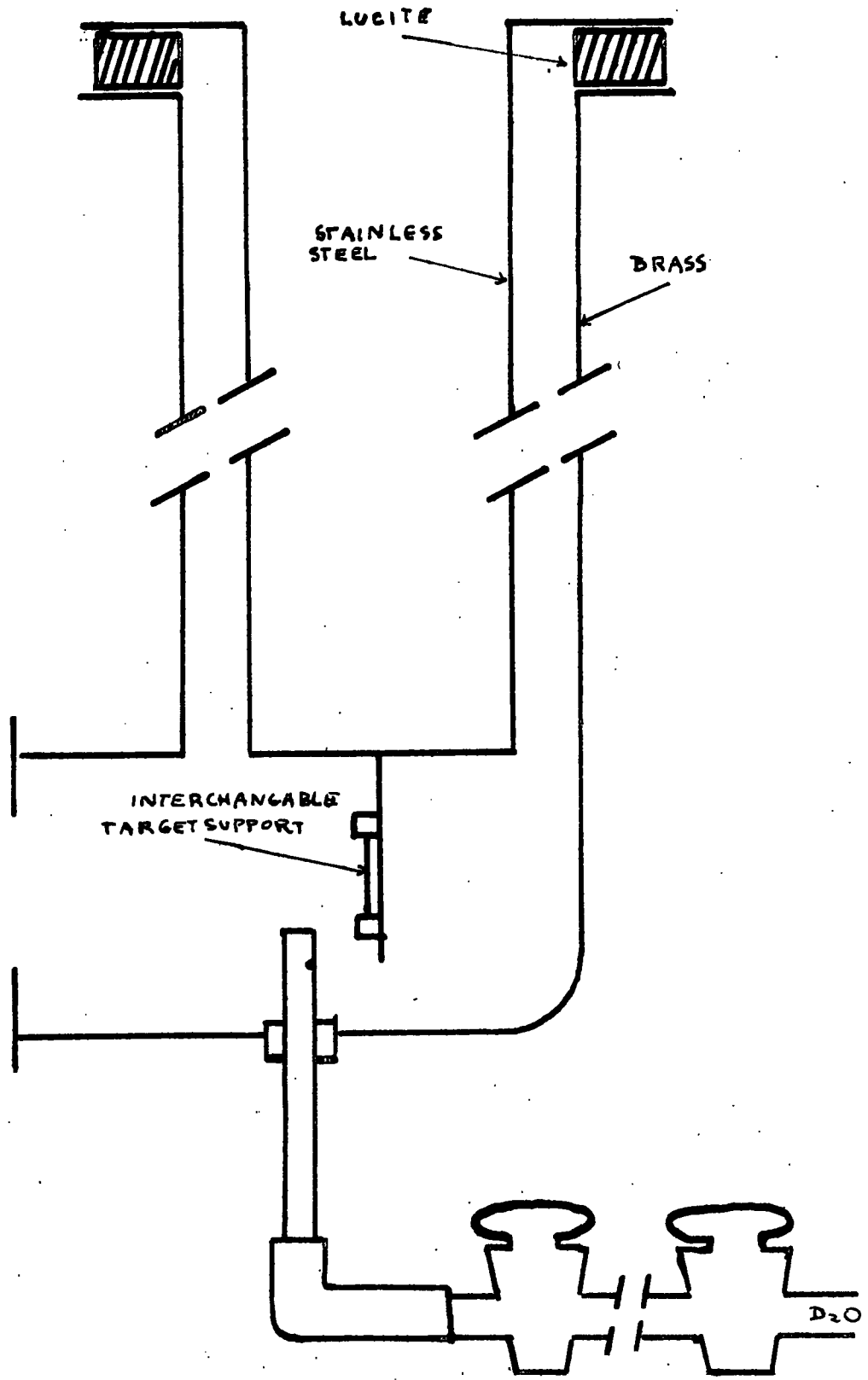

FIG. 8: Target Arrangement.

calculated for equation (2)

$$T = e^{-N\sigma x}$$

or $$- \log T = - 0.435 \sigma \ln T = 0.435 N \sigma x$$

where x is the length of the absorber, σ the total cross section of N^{14}, and N is the total number of nitrogen atoms per unit volume. N may be expressed as

$$N = \frac{A \cdot \rho}{W} = \frac{(6.02)(10^{23})(0.808)}{14} = 3.46(10^{22})$$

where A is Avogadro's number, ρ the density of liquid nitrogen, and W the atomic weight of nitrogen. Assuming the cross section to be 1.5 barn the absorber length will be

$$x = \frac{- \log 0.5}{(1.5)(10^{-24})(3.46)(10^{22})} = 14 \text{ cm}$$

The length of the absorbers thus was chosen to be 15 cm, which gives for these absorbers the relationship between transmission and cross section as

$$\sigma = \frac{- \log T}{(0.435)(3.46)(10^{22})(15.0)} = - 4.44(10^{-24}) \log T$$

or $$\sigma = - 4.44 \log T \text{ (barn)}$$

This relation was plotted on semi log paper to permit fast conversion of transmission into cross section values (Fig. 7).

3. Target.

Since neutrons of energies above 3.5 Mev were required the neutrons were obtained from the $D^2(d,n)He^3$ reaction. A heavy ice target was used, as sketched in Fig. 8. The target was deposited in the following way. The lower tap was opened until the manometer read 1.2 cm Hg, then the lower tap was

To follow page 38

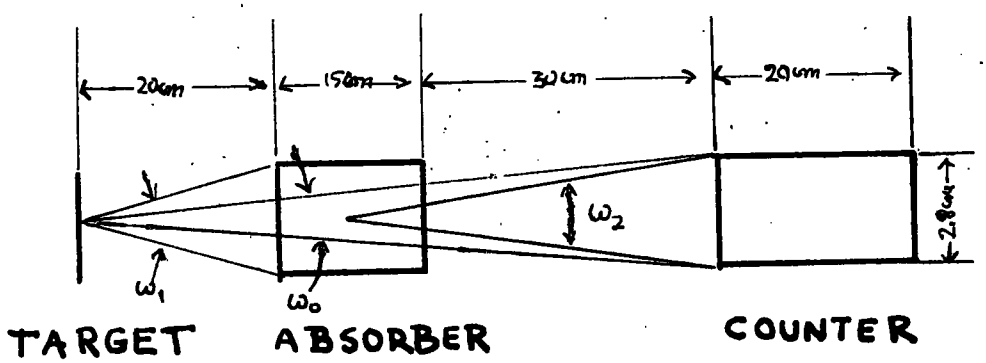

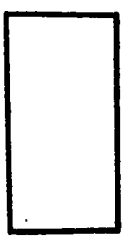

MONITOR

FIG.9: General Arrangement and Geometry of the Experiment.

closed and the upper opened until the manometer read zero pressure.

The thickness of a target produced by such a system may be estimated. Since 22.4 liters of D_2O at atmospheric pressure would weigh 20 grams, the amount of D_2O contained in 50 cm^3 at 1.2 cm Hg will be

$$\frac{(20)(1.2)(50)}{(22.4)(76)(1000)} = 7.1(10^{-4}) \text{ gms of } D_2O$$

Assuming about one half of this deposits on the target we obtain for a 4.7 cm^2 target a thickness of $7.6(10^{-2})$ mg per cm^2. Taking the stopping power of D_2O to be

$$8(10^{-15}) \text{ ev-cm per molecule}$$

or $$\frac{(8)(10^{-15})(6)(10^{23})}{20} = 0.24 \text{ mev per mg}$$

we find that the stopping power of the target is

$$(7.6)(10^{-2})(0.24) = 1.8(10^{-2}) \text{ mev/cm}^2$$
$$= 18 \text{ kev/cm}^2$$

4. Geometrical Considerations.

Fig. 9 illustrates the geometry of the experiment. Assuming the solid angles small, we find

$$\omega_1 = \frac{2.8}{20} = 0.125$$

$$\omega_2 = \frac{2.8}{3.5} = 0.067$$

$$\omega_o = \frac{2.8}{65} = 0.039$$

Substituting these values into equation (7), the geometrical factor is

$$G = \frac{(0.125)(0.067)}{2\ 0.039} = 4.7(10^{-2})$$

and if we assume a measured transmission of 0.5, the true

transmission will then be from equation (8)

$$T = T_o + (1 - T)\, G = 0.5 + 0.5G = 0.523$$

which gives us an error due to geometry of

$$\Delta\frac{T}{T} = \frac{T_o - T}{T} = 4.7(10^{-2}) = 4.7\%$$

This appeared to be below the expected statistical errors.

To calculate the expected counting rate the expected target yield for 4 Mev neutrons and a solid angle of $\omega_o = 0.042$ in the forward direction must first be calculated. The target yield is given by

$$n = n_o\, tN'$$

where n_o is the number of incoming deuterons per second. Assuming a beam current of I = 10 microamperes, we have

$$n_o = \frac{I}{\text{charge of an electron}} = \frac{10^{-5}}{1.6(10^{-19})} = 6.4(10^{13})$$

N' is the number of D atoms per mg of target,

$$N' = 2\frac{A}{W} = 2\,\frac{6(10^{23})}{20} = 6(10^{22}) \text{ per gm}$$

$$= 6(10^{19}) \text{ per mg}$$

and t is the thickness of the target in mg per cm^2. It was found on page 39 that t is approximately 0.2[illegible] mg per cm^2 for a 20 kev target.

In order to estimate the cross section for neutrons emerging in solid angle from θ_1 to θ_2, we must integrate the differential cross section over that region. As mentioned in chapter IV, the differential cross section for D-D neutrons is given by

$$\sigma = A + B\cos^2\theta + C\cos^4\theta$$

Thus the total cross section for neutrons between the angles θ_1

and θ_2 will be

$$\sigma_{1,2} = \int_{\theta_1}^{\theta_2} \sigma \, d\theta$$

$$= (A + \frac{B}{2} + \frac{3}{8}C)\,\theta\Big]_{\theta_1}^{\theta_2} + (\frac{B}{2} + \frac{3C}{8})\cos\theta \sin\theta\Big]_{\theta_1}^{\theta_2}$$

$$+ \frac{3C}{8}\cos^3\theta \sin\theta\Big]_{\theta_1}^{\theta_2}$$

Assuming $\sin\theta = \theta$ and $\cos\theta = 1$, this expression will reduce to

$$\sigma_{1,2} = (A + B + \frac{9}{8}C)\,\theta\Big]_{\theta_1}^{\theta_2}$$

The three constants can be estimated for 1 Mev deuterons from curves published by Graves (1952)

$$A \approx 4\ (10^{-27})\text{cm}^2,\ B \approx 1.4(10^{-27})\text{cm}^2,\ C \approx 1.6(10^{-27})\text{cm}^2$$

and we obtain for the cross section in the forward direction, at a solid angle of $\omega_0 = 0.04$

$$\sigma \cong (4 + 1.4 + 1.8)(10^{-27})(0.04) = 1.3(10^{-28})\text{cm}^2$$

The target yield then will be

$$n = (6.4)(10^{13})(1.3)(10^{-28})(6)(10^{19})(5)(10^{-2})$$

$$= 2.5(10^4) \text{ neutrons/sec}$$

Assuming a counter yield of 0.45%, as calculated on page 37, a counting rate is thus obtained of

$$n' \cong (2.5)(10^4)(4.5)(10^{-3}) = 110 \text{ counts/sec}$$

$$= 6.6(10^3) \text{ counts/min}$$

5. Energy Control System.

In order to obtain resonances in the energy dependence of the cross section the energy resolution must be good, and the energy of the beam must be stable and accurately known. The system used for controlling the beam energy of the U.B.C.

To follow page 41

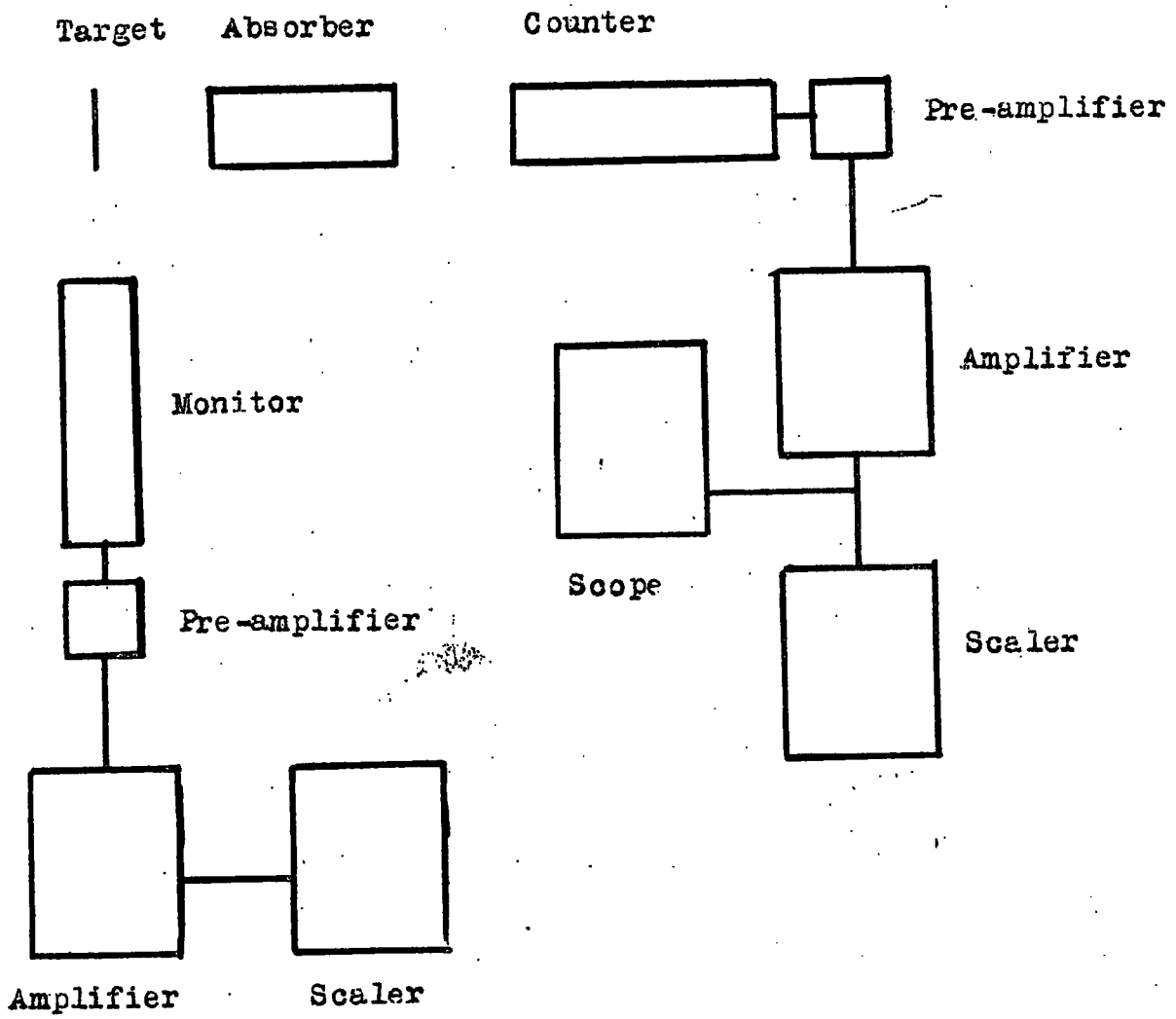

FIG. 10: Blockdiagram of the Electronics of the Experiment.

Van de Graaf generator is described by Aaronsen (1952). The deuteron energy was maintained to ±3 kev during the runs made for this experiment, using a reverse electron beam control system.

The neutron energy may be obtained from

$$3Q = 4E_n - E_\alpha - 2\cos\theta(2E_dE_n)^{1/2} \quad \ldots\ldots\ldots(29)$$

6. Electronic System.

Fig. 10 is a block diagram of the electronic system employed in this experiment. The counter and the monitor pulses were each connected through a head amplifier and a linear amplifier to a scaler. The individual components that were employed are:

E.K. Cole Amplifier Unit Type 1049 B,

Atomic inst. Linear Amplifier Model 204-B,

Lambda Power Supply Model 28,

Northern Electric Fast Linear Amplifier AEP 1444,

Marconi Pulse Height Analyser AEP 516,

Dynatron Radio Scaler Type 1009 A.

To follow page 42

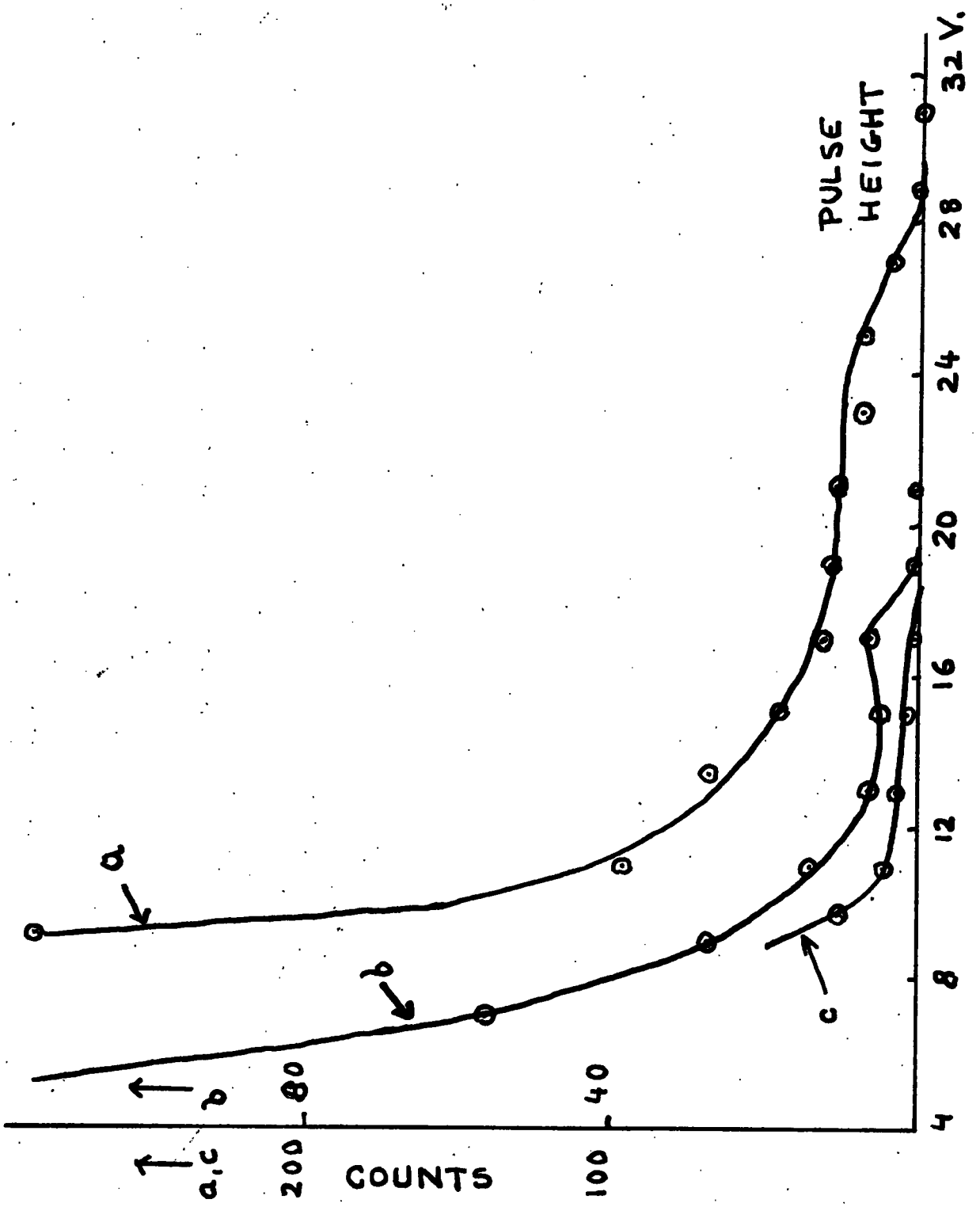

FIG.11: Pulse Height Distribution of the Propane Recoil Counters: (a) E_n = 4.2 Mev; (b) E_n = 2.9 Mev; (c) Background Counts.

To follow page 42

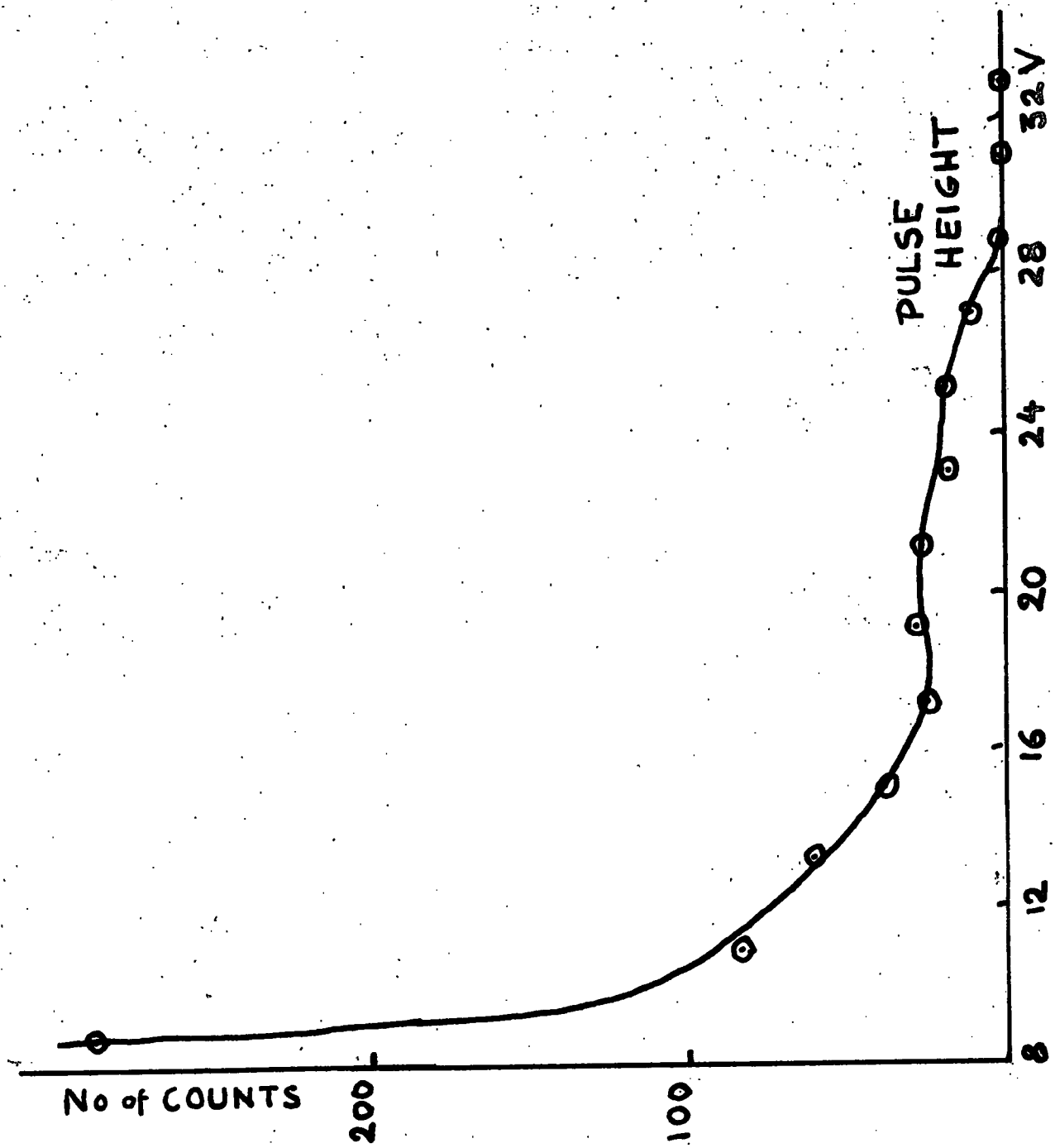

FIG.12: Pulse Height Distribution of a Propane Counter; background subtracted (E_n = 4.2 Mev)

VI. EXPERIMENTAL PROCEDURE

1. Test of the Counters.

The counters were first tested with a 50 mc Ra-Be source and the proportional region was found to be around 3000 volts. The background counting rate was found to be excessive. This was traced down to break-down on a piece of Bakelite, which was used to support the filter of the H.T. input. After the Bakelite had been replaced by Lucite, the background without any source in the vicinity was found to be practically zero for one counter, and of the order of 10 counts per minute for the other. This must presumably have been due to chemical contamination or possibly alpha contaminations from the walls. The counters were then irradiated with 3.9 and 4.2 Mev monochromatic neutrons, and their pulse height distributions were recorded on an eighteen channel pulse height analyser. Both counters showed the same distribution, although the operating voltage for the same gas amplification was not quite the same. Typical distributions are shown in Fig. 11. The background due to scattered neutrons and gamma rays was measured by inserting 7.5" of paraffin between the target and the counter (Fig. 11c). Fig. 12 shows a typical distribution from which the background was subtracted. This may be compared with the pulse distribution calculated distribution mentioned on page 35 and shown on Fig. 6. Although the experimental distributions are not quite in agreement with the calculated they are very similar to those obtained experimentally by Skyrme, Tunnicliffe and Ward (1952)

with their methane counter.

By varying the operating voltage it was found that the change in gas amplification was approximately a factor of two for 200 volts. The absolute gas amplification was measured by the following simple test pulse generator. A 1.5 volt battery was connected to a resistor chain through a mercury switch which was fastened on a pendulum. The pulse height was determined by a voltmeter and the known attenuation of the resistor chain, which was connected through a coupling capacitor to the head amplifier. The attenuation was adjusted until pulses were obtained of the same height as pulses from 4 Mev recoil protons. For one counter it was found that the required pulse voltage was $7.34(10^{-2})$ volts. Having a coupling capacitor of 10 micro-microfarad, it may be assumed a charge of $Q = vc = (7.34)(10^{-2})(10^{-11}) = 7.34(10^{-13})$ coulomb produces a pulse equivalent to that of a 4 Mev proton. Since, on the other hand, the energy loss per ion pair is 33 ev, a primary charge of $1.2(10^{5})$ ions per 4 Mev proton will be produced, or $Q_o = 1.9(10^{-14})$ coulombs per proton. Thus the gas amplification will be

$$A = \frac{Q}{Q_o} = \frac{7.34(10^{-13})}{1.9(10^{-14})} = 39$$

In a similar way it was found that the gas amplification for the other counter was 30. The ratio 39 to 30 checks well with the ratio of the output voltages of the main amplifier for the two counters, which was 44 to 34. These gas amplification values are of the same order of magnitude as one would expect from Rossi and Staub's (1949) curves for methane.

To follow page 44

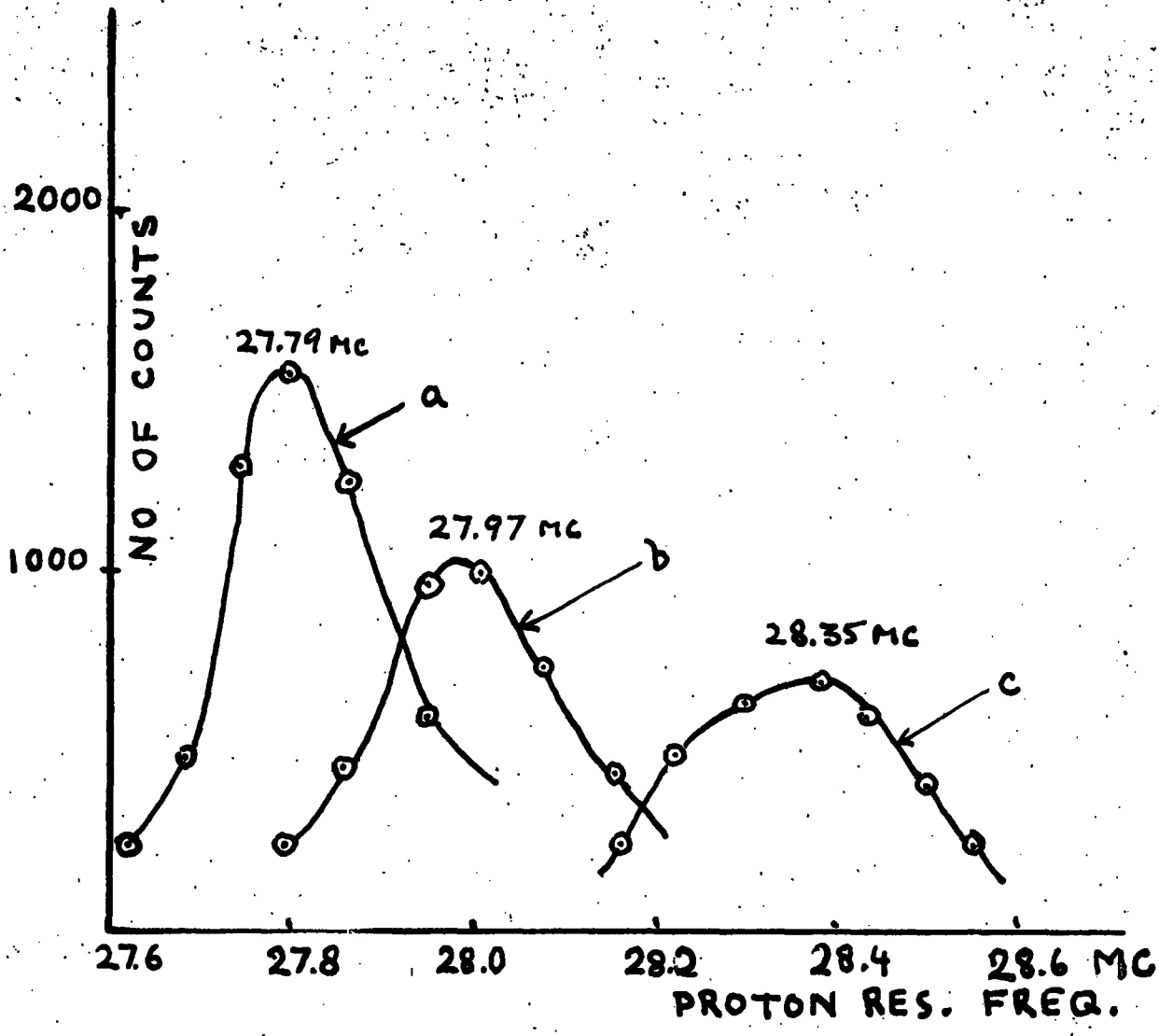

FIG.13: $F^{19}(n,\gamma)$ 0.873 Mev Resonance: (a) with no deuterium target superimposed, (b) with one deuterium target superimposed, (c) with two deuterium targets superimposed.

To follow page 44

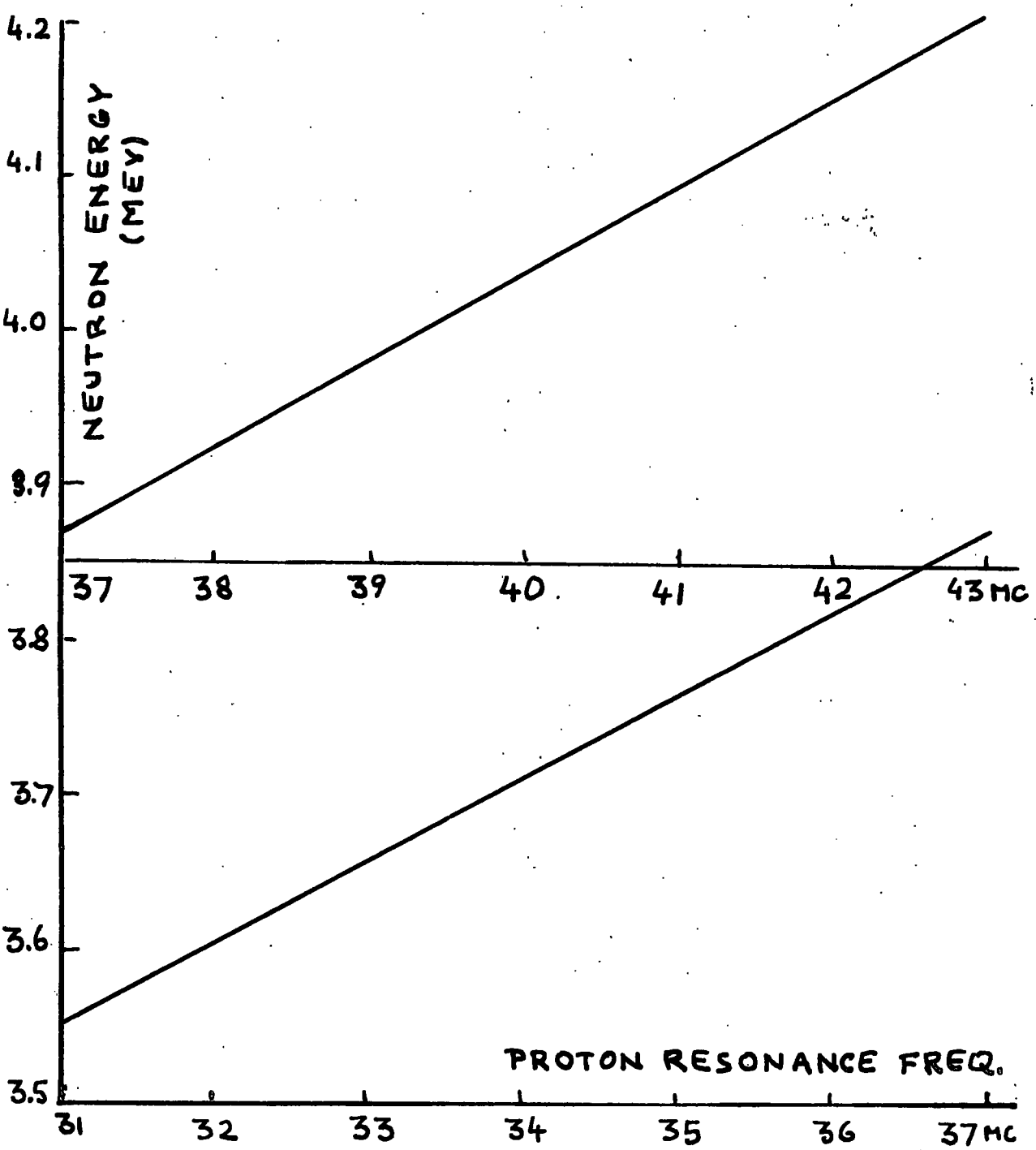

FIG.14: Neutron Energy vs. Proton Resonance Frequency for the Energy Control System Employed.

2. Calibration of the Energy Scale and Measurement of the Target Thickness.

To calibrate the energy scale the 0.873 Mev resonance of the $F^{19}(p,\gamma)Ne^{20}$ was measured. This resonance has been measured accurately by Aaronsen (1952). The present measurement was carried out in a manner similar to that of the latter. A thin fluorine target and a gamma ray scintillation counter, which were available in this laboratory, were used for the measurement. As Fig. 13a illustrates, the resonance was found to be at a proton resonance frequency of 27.79 megacycles per second. Thus the relation between proton energy and proton resonance frequency can be expressed as

$$873.5 \text{ kev} = k_p \, (27.79\text{mc})^2$$

or

$$k_p = 1.141 \text{ kev/mc}^2$$

where k_p is the energy calibration constant for protons. Since, with a constant magnetic field and a constant beam deflection, the beam energy is inversely proportional to the mass of the ions, the energy calibration constant for deuterons will be

$$k_D = \frac{k_p}{2} = 0.571 \text{ kev/mc}^2$$

From this the deuteron energy was calculated for different frequencies from 31 to 43 mc. Substituting these values into equation (29) of the last chapter, the neutron energies corresponding to the different proton resonance frequencies were obtained and a calibration curve of neutron energy as a function of proton resonance frequency was plotted. This curve is illustrated in Fig. 14.

The energy thus having been calibrated, the target

thickness of one "scoop" D_2O (i.e. 50 c.c. D_2O at 1.2 cm Hg) was measured the following way. A one "scoop" D_2O target was superimposed on the fluorine target, and the fluorine resonance was measured again. The resonance was found to be at 27.97 mc (Fig. 13b). Another target was added, and the resonance was found to be at 28.35 mc (Fig. 13c). The energies for these frequencies were calculated with the help of the above k_p to be 915 and 930 kev respectively. Thus a target of 50 c.c. D_2O at 1.2 cm Hg was found to be 15 kev thick for protons of 0.8 Mev energy. Assuming that the stopping power for deuterons is twice that for protons, such a target will have a thickness of 30 Mev for deuterons of 0.8 Mev energy.

3. Test of the Absorber Dewars.

In order to ensure that all three absorber Dewars were equivalent, and that their absorptions therefore cancelled, the transmission of each of the three containers was measured. This was done by comparing the counting ratio with the Dewar in place with the counting ratio with the Dewar removed. The transmissions were found to be 0.763, 0.622 and 0.630. Since this is a relatively low transmission and since one of the Dewars showed quite a discrepancy, the side walls of the Dewars were thinned as far as it was mechanically possible. This improved the transmissions to values of 0.922, 0.918 and 0.876. It was thus decided to use the Dewar with the slightly different transmission with water as an absorber, so that this discrepancy would not influence the results.

4. Counting Rate and Counting Period.

It was found that with a 12 kev target the counting rate was of the order of 3000 counts per minute for a 12 microamp. beam. The estimate in the last chapter gave 6600 counts per minute for a 20 kev target and 10 microamps, which would give $\frac{(6600)(12)(12)}{(20)(10)}$ = 4700 counts per minute under the above conditions. Thus the calculated and the measured counting rates were in fair agreement. That they are not in complete agreement was to be expected, since in the estimate a theoretical counter efficiency was used, and since the ion beam is never quite constant.

Because of the instability of the beam it was decided to control the counting periods for the different measurement by means of a current integrator rather than with a clock. To decide on the most suitable counting period for each of the three different runs on one energy point, i.e. the nitrogen run, the water run and the run with no absorber, preliminary measurements of the counting ratios were made. It was found that the counting ratios for the different absorbers were roughly: for no absorber $r_o = 0.90$, for nitrogen $r_1 = 0.50$, and for water $r_2 = 0.25$. Inserting these into the expression given in chapter I for the statistical error (equation 9), we obtain

$$\frac{\Delta\sigma}{\sigma} = \frac{1}{\ell nT}\left[16\, r_1^2 + 6.25\, r_2^2 + 6.25\, r_o^2\right]^{\frac{1}{2}}$$

This indicates that the nitrogen run has twice as much influence on the statistics than each of the two other runs. Thus it was decided to count on the nitrogen runs twice as long as

To follow page 47

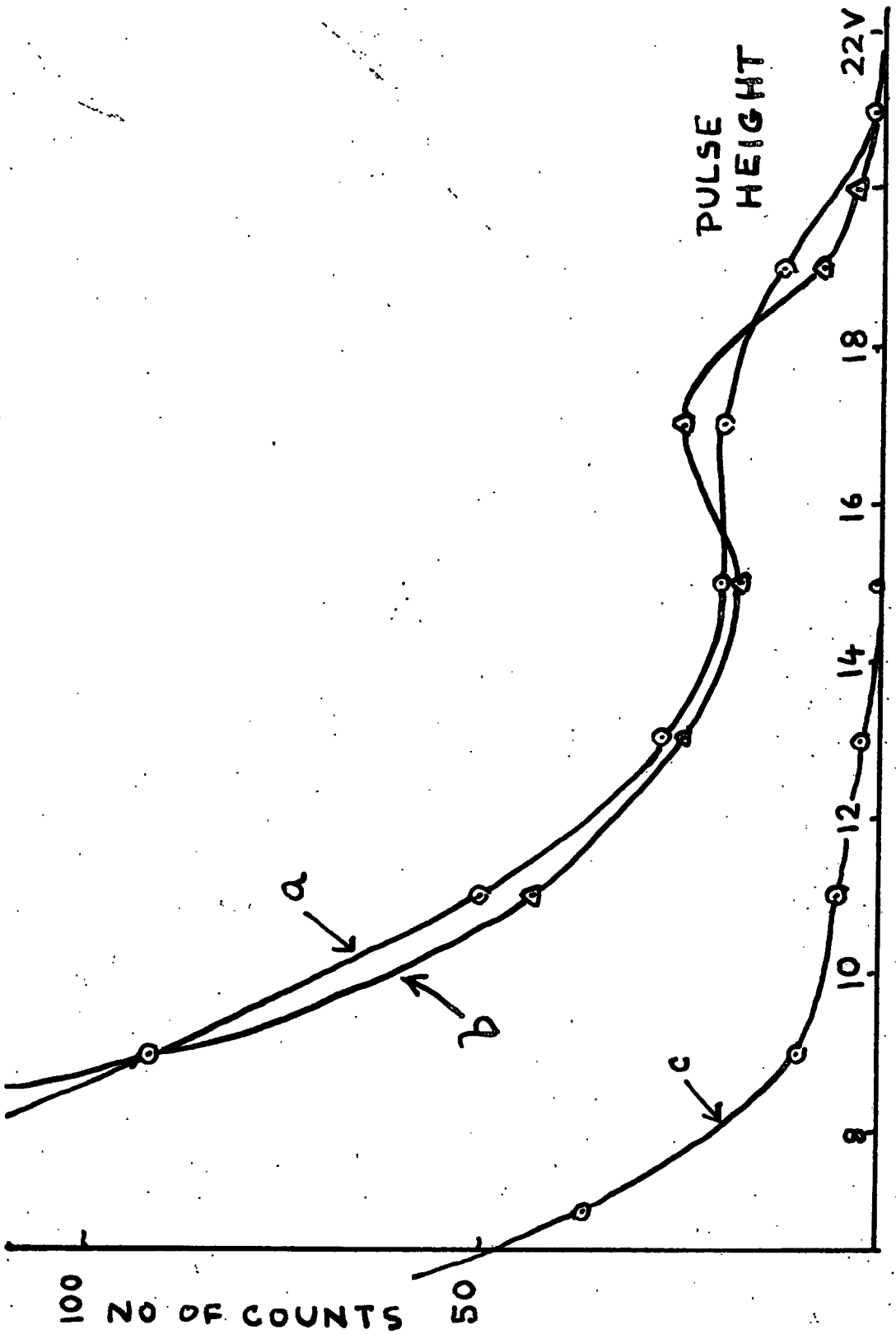

FIG.15: Target Neutron Background: (a)Dirty target; (b) Cleaned target; (c) Thick carbon target.

on the other ones.

5. Measurement of the Parasitic Neutron Background.

Since the D(d,h)He reaction produces only one group of monochromatic neutrons no parasitic neutrons from the target itself were expected, while it was assumed there would be some neutrons coming from carbon contamination of the target and deuterium contamination of the target support. As the amount of such contamination would depend on the time that the target had been exposed, the corrections as discussed in chapter I could not be applied. Thus all efforts concentrated towards reducing these neutron components.

To be able to distinguish between the two types of background, a thick carbon target was prepared by applying some aquadac to a copper sheet. Then a heavy ice target was bombarded for several hours, while the preliminary runs for the cross section measurement were done. When the target looked nicely dirty, the heavy ice was evaporated and the pulse spectrum of the dirty target support was measured (Fig. 15a). The support was then buffed thoroughly until all the dirt was removed, and was afterwards cleaned thoroughly with carbon tetrachloride. The pulse spectrum of the cleaned target is shown on Fig. 15b. Then the carbon target was inserted and its pulse spectrum measured. (Fig. 15c). A comparison of these three curves seems to indicate that the large background is due to deuteron contamination in the target backing support. That the contaminated deuterons give neutron energies of about 400 kev lower than the ice target is presumably due

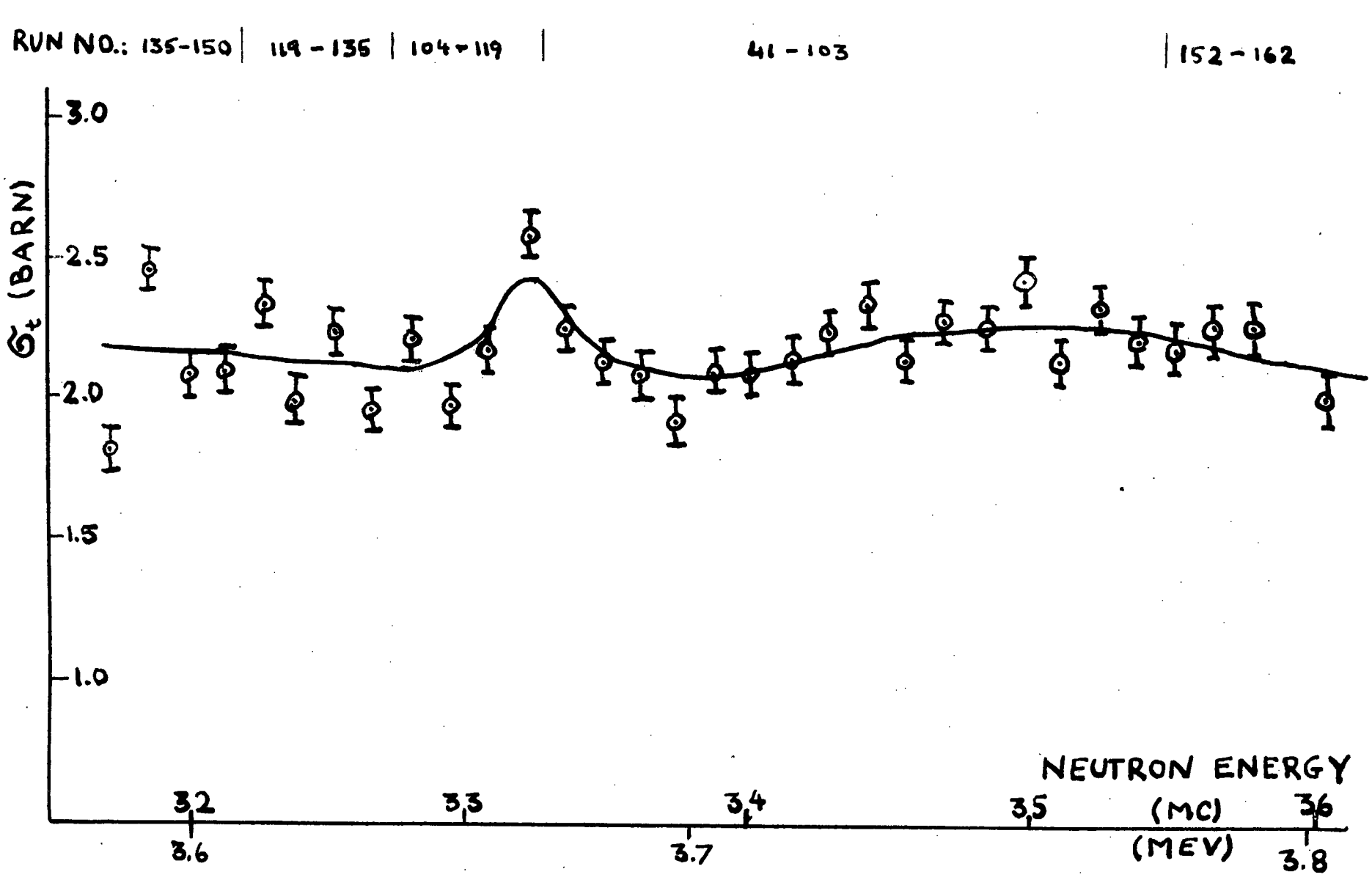

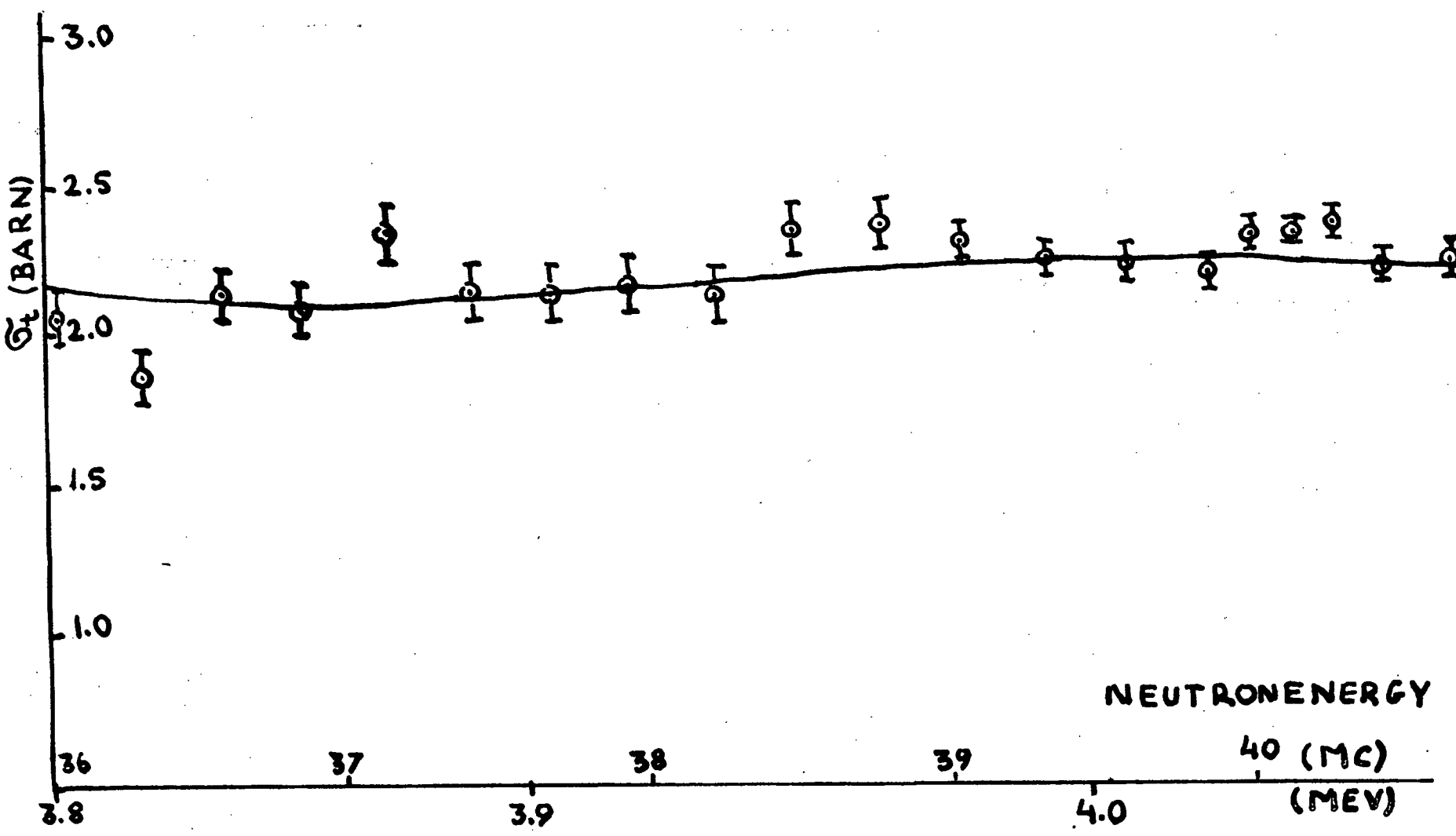

FIG.16: The Total Cross Section of N^{14} at Neutron Energies from 3.6 t o 4 Mev.

to stopping of the beam by the target support, before it reaches the deuterium. To ensure that this argument is right, and to have an estimate of the strength of the background, the following were measured under the same beam conditions:

a) Dirty heavy ice target, 600 counts per 15 integrator counts.

b) The same target support, the heavy ice evaporated, 351 counts per 15 integrator counts.

c) A new target support, made from the same sheet of copper as the other, 80 counts per 15 integrator counts.

Thus, the background, after long bombardment of the target, was up to 50% of the counting rate, was due to deuterium absorption by the target support, and was approximately 400 kev lower in energy than the desired neutrons. Since there seemed no way of eliminating this background completely it was decided to minimize it by changing the target support after each six points of cross section measurement.

6. Measurement of the Cross Section.

The cross section was measured for neutron energies from approximately 3.6 to 4.1 Mev. The results are plotted in Fig. 16 as a function of energy. To illustrate how these results were achieved, Table II lists the readings of a typical point.

The neutron energy and the cross section value were read from curves similar to Figs. 14 and 7 respectively. The statistical errors were calculated with the help of equation (9). First, however, the errors of the individual counting ratios were calculated. If x is the number of counts on the counter

Table II

Readings of a typical point of measurement

Absorber	Time sec	Integrator counts	Monitor counts	Counter counts	Counting ratio
Air	117	25	5507	7090	1.288 = r_o
H_2O	119	25	5646	1465	0.259 = r_2
N_2	107	25	5756	3567	0.620
N_2	113	25	5652	3315	0.587 — 0.603 = r_1

Proton resonance frequency: 33.202 mc E_n = 3.671 Mev

Generating voltmeter: 675 kev

Target current: 12 microamps

Transmission: $T = \frac{0.603 - 0.259}{1.288 - 0.259} = 0.334$ σ = 2.16 barn

and y is the number of counts on the monitor, we obtain for the error of the nitrogen counting ratio in the example of Table II

$$\Delta r_1 = \left[\frac{x_1 + y_1}{x_1 y_1}\right]^{\frac{1}{2}} r_1 = \left[\frac{3964 + 8252}{(3964)(8252)}\right]^{\frac{1}{2}} 0.481 = 0.0102$$

Similarly we get for the water counting ratio

$$\Delta r_2 = \left[\frac{1118 + 4293}{(1118)(4293)}\right]^{\frac{1}{2}} 0.261 = 0.00876$$

and with no absorber

$$\Delta r_o = \left[\frac{3884 + 3990}{(3884)(3990)}\right]^{\frac{1}{2}} 0.948 = 0.0206$$

and to calculate the error in cross section we find

$$\left[\frac{\Delta r_o}{r_o - r_1}\right]^2 = \left[\frac{(2.06)(10^{-2})}{-.467}\right]^2 = 1.92(10^{-3})$$

$$\left[\frac{\Delta r_1}{r_1 - r_2}\right]^2 = \left[\frac{(1.02)(10^{-2})}{0.220}\right]^2 = 2.15(10^{-3})$$

$$\left[\frac{\Delta r_2(r_o - r_1)}{(r_1 - r_2)(r_o - r_2)}\right]^2 = \left[\frac{(8.76)(10^{-3})(0.467)}{(0.220)(0.687)}\right]^2 = 0.733\ (10^{-3})$$

and the fractional error then is

$$\frac{\Delta\sigma}{\sigma} = \frac{1}{\ell n 0.318}\left[19.2 + 21.5 + 7.3\right]^{\frac{1}{2}}\ (10^{-2})$$

$$= 0.059 = 5.9\%$$

VII. DISCUSSION OF RESULTS

Only one resonance has so far been measured in this energy region by other workers (c.f. chapter II, section 2d). It was reported as being questionable because the measurement was undertaken with continuous neutron energies and therefore may have been caused by a transition into an excited state of B^{11}. Its position was reported at a neutron energy of 3.7 Mev. This would coincide approximately with the small peak in cross section on Fig. 16. However, although the statistics obtained might justify the assumption that there is a resonance, the instability of the points below that energy makes it rather doubtful. This instability must presumably have been due to some instability in the energy control system.

It may thus be concluded that the present measurements neither confirm nor deny the resonance reported at 3.7 Mev by Stetter and Bothe (1951). The fact that there appears to be no resonance between 3.7 and 4 Mev, according to Stetter and Bothe, seems confirmed by the present experiment.

BIBLIOGRAPHY

D. Aaronsen, Thesis, 1952, University of British Columbia.

Ajzenberg and Lauritzen, 1952, Revs. Mod. Phys., 24, 321.

Baldinger and Huber, 1938, Helv. Phys. Acta, 11, 245.

Barshall and Bethe, 1947, Rev. Sci. Inst., 18, 147.

Bollman and Zunti, 1951, Helv. Phys. Acta, 24, 517.

Caldwell and Armstrong, 1952, Rev. Sci. Inst., 23, 508.

Collins, 1948, Phys. Rev., 73, 1543.

Deutsch, M.I.T. Technical Report No. 3.

Feld, Feshbach, Goldberger, Goldstein and Weisskopf, 1951, "Final Report of the Fast Neutron Project" USAEC, Report No. NYO-636-January 31.

Feshbach, Peaslee and Weisskopf, 1947, P.R.71, 145.

Graves et al., Nucl., 1952, 10, 68, December.

Graves and Froman, editors, 1952, "Miscellaneous Physical and Chemical Techniques of the Los Alamos Project", McGraw-Hill.

Halliday, 1950, "Introductory Nuclear Physics", Wiley.

Hinchley, Stelson and Preston, 1952, P.R.86, 483.

Huber et al., 1949, Helv. Phys. Acta, 22, 418.

Humber and Richards, 1949, Phys. Rev., 75, 335A.

D.B. James, Thesis, 1953, Cambridge Unitersity.

James, Kubelka, Heiberg and Warren, 1955, Can. J. of Phys. "to be published".

Johnson, Patree and Adair, 1951, P.R.84, 775.

Kallman, 1947, Natur und Technik, Juli.

Keeping and Lovberg, 1952, Rev. Sci. Inst., 23, 483.

Korff, 1947, "Electron and Nuclear Counters", Van Nostrand.

Krebs, 1953, Erg. Ex. Naturw., 27, 379.

Livingstone and Bethe, 1937, 9, 269.

Marshall and Coltman, 1947, Phys. Rev., 72, 528.

Moon, 1948, Phys. Rev., 73, 1210.

Ricamo, 1951, Nuovo Cim., 8, 383.

Ricamo and Zunti, 1951, Helv. Phys. Acta, 24, 419.

Ricamo and Zunti, 1951, Helv. Phys. Acta, 24, 302.

Rose and Shapiro, 1948, Phys. Rev., 74, 1853.

Rossi and Staub, 1949, "Ionization Chambers and Counters", McGraw-Hill.

Schenck, 1952, Nucl., 10, 54, August.

E. Segre, editor, 1953, "Experimental Nuclear Physics", Vol. I.

Skyrme, Tunnicliffe and Ward, 1952, Rev. Sci. Inst., 23, 204.

Stetter and Bothe, 1951, Z. Naturfschg., 6a, 61.